ABSTRACT

Title of Thesis: **OCULAR BARRIERS TO TRANSSCLERAL DRUG DELIVERY AND PHARMACOKINETICS OF AN EPISCLERAL IMPLANT**

Susan Shu-Hsun Lee, Master of Science, 2006

Directed By: Professor Nam Sun Wang
Department of Chemical Engineering
Bioengineering Graduate Program

The eye presents several anatomic and physiologic barriers that pose a major challenge for targeted drug delivery. The primary causes of vision impairment and blindness result from posterior segment diseases and corneal diseases[1]. To tackle these sight-threatening diseases, a number of therapeutic methods have been investigated, ranging from topical eye drops to injections and implants. Thus, the development of effective delivery systems depends upon the understanding of how the ocular barriers affect the pharmacokinetics of drugs. In Part 1, investigation of the barriers to transscleral drug delivery was performed in a rabbit model, and the model demonstrated that the conjunctival lymphatic and blood vessels may be a predominant barrier to the delivery of triamcinolone acetonide to the vitreous. In Part 2, the pharmacokinetics of a cyclosporine episcleral implant for high-risk penetrating keratoplasties was also studied, and the implant was safe and effective at delivering therapeutic levels to the cornea and surrounding tissues.

OCULAR BARRIERS TO TRANSSCLERAL DRUG DELIVERY AND PHARMACOKINETICS OF AN EPISCLERAL IMPLANT

By

Susan Shu-Hsun Lee

Thesis submitted to the Faculty of the Graduate School of the
University of Maryland, College Park, in partial fulfillment
of the requirements for the degree of
Master of Science of
Bioengineering
2006

Advisory Committee:
Professor Nam Sun Wang, Chair
Professor William Bentley
Professor Adam Hsieh
Professor Srinivasa Raghavan

List of Tables

List of Figures

Chapter 1: Introduction

The main goal of ocular drug delivery is controlled release of therapeutic concentrations to specific tissues while avoiding systemic spread of the formulation. However, the eye presents several anatomic and physiologic barriers that pose a major challenge for targeted drug delivery, especially to the posterior segment. The primary causes of vision impairment and blindness result from posterior segment diseases and corneal diseases [1]. To tackle these sight-threatening diseases, a number of therapeutic methods have been investigated, ranging from topical eye drops to injections and implants. Thus, the development of effective delivery systems depends upon the understanding of how the ocular barriers affect the pharmacokinetics of drugs.

Overview of Eye Anatomy

The eye has two segments - a smaller, transparent anterior segment that makes up one-sixth of the eyeball, and an opaque, posterior segment that forms the remaining five-sixths of the eyeball (Figure 1-1)[2].

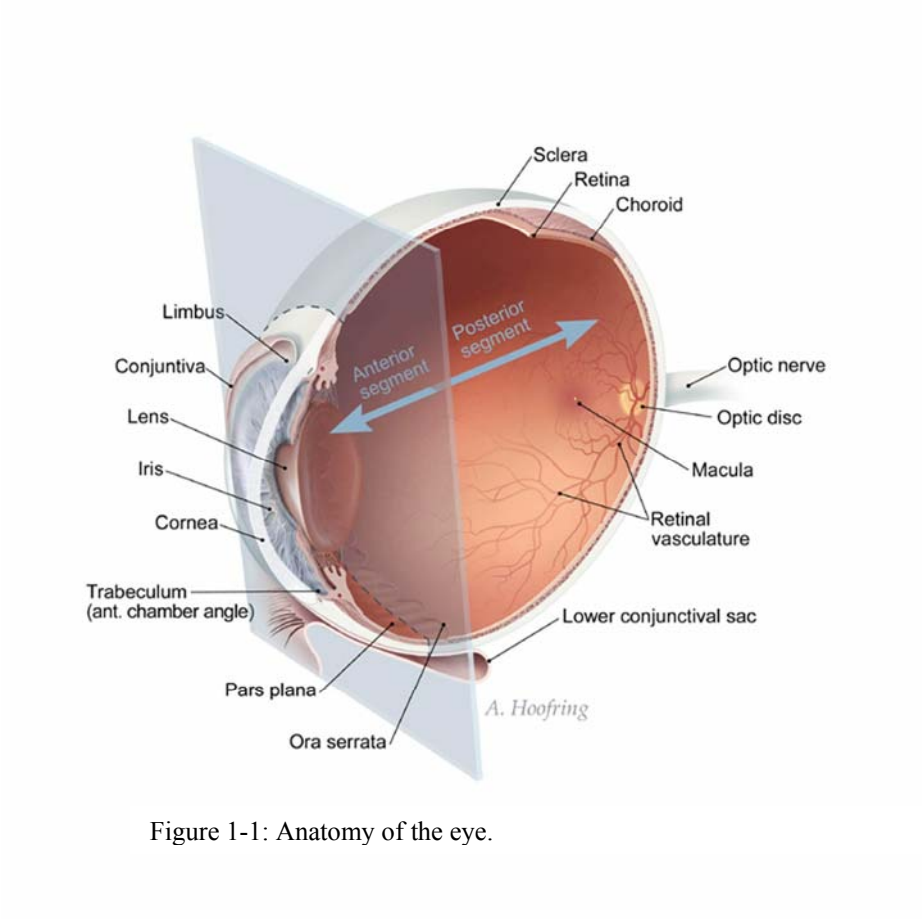

Figure 1-1: Anatomy of the eye.

Anterior Segment

Conjunctiva

The conjunctiva is a thin transparent mucous membrane that lines the inside of the eyelids and is reflected onto the anterior one-third of the eyeball. The lining of the eyelids are referred to as palpebral conjunctiva and the eyeball layer as bulbar conjunctiva. The transitional region, where the palpebral conjunctiva is reflected to become the bulbar conjunctiva and forms a sac, is called the fornix. The conjunctiva is composed of two cellular layers, an epithelial layer and an underlying stromal layer. The epithelial cells are connected by tight junctions that form a permeability

barrier, especially for hydrophilic compounds that are transported paracellularly [3]. The stroma contains structural and cellular elements, including lymphatic vessels, blood vessels, and nerves. The conjunctiva is loosely attached to the underlying sclera.

Cornea

The transparent cornea is the main structure responsible for light refraction, and its curvature is greater than the rest of the globe. At the circumference of the cornea is the limbus, where the cornea becomes continuous with the sclera and the conjunctiva. Three cellular layers compose the cornea – the superficial epithelium, the thickest and most fibrous stroma, and the single-layered endothelium. The epithelial cells are connected by tight junctions, similar to conjunctival epithelial cells, and also hinder movement of hydrophilic compounds [4]. This barrier represents the principle barrier to transcorneal transport. Moreover, corneal permeability to hydrophilic molecules is one order of magnitude lower than the conjunctiva. The transport of lipophilic compounds is the converse, where the permeability of the cornea increases with increasing lipophilicity [5].

Iris and Lens

The iris is a thin, circular, contractile diaphragm that controls the amount of light refraction through the lens, depending on the brightness of the environment [2]. It is pigmented and the central aperture forms the pupil. The anterior surface of the biconvex transparent lens presses lightly against the iris. The lens is responsible for

adjusting its dioptric power to allow distant and near objects to be focused on the retina.

Trabeculum, Pars Plana, Ora Serrata

The trabeculum is a meshwork of canals which function in the drainage of the anterior chamber to the circulation. The angle formed by the trabecular meshwork, cornea, and iris is important for evaluating glaucoma. The pars plana is the smooth and flat posterior surface of the ciliary body, a fibrous and muscular tissue that is continuous anteriorly with the peripheral margin of the iris and continuous posteriorly with the choroid. Near the pars plana is the ora serrata, the anterior margin of the retina where the nervous tissues end. Intravitreal injection of drugs and surgery are commonly performed through the pars plana due to its relative avascularity and anterior position to the retina [2, 6].

Posterior Segment

Sclera

The sclera is the opaque fibrous layer covering the posterior five-sixths of the eyeball, and functions to protect the intraocular contents of the eye. It is mainly composed of collagen, and a sparse population of fibroblasts, proteoglycans, and a few elastic fibers [7]. The avascular sclera is continuous with the cornea at the limbus. The anterior part of the sclera forms the "white" of the eye and is covered with the fibrous tissue of Tenon's fascia and the conjunctiva. The episclera, the outermost layer of the sclera, and Tenon's fascia form a potential space called the episcleral space. Scleral

permeation occurs through pores between the fibers and intracellular spaces, and permeability has been shown to depend more on molecular radius than lipophilicity [5] [8] [9]. Transscleral drug delivery to posterior segment targets have been investigated because the sclera is significantly more permeable than the cornea [4].

Choroid

The choroid is a thin vascular tissue that lines the inner surface of the sclera. It extends from the optic nerve posteriorly to the ciliary body anteriorly, where it gradually thins. The function of the choroid is to nourish the outer layers of the retina with its blood vessels.

Vitreous Humor

The vitreous is a colorless, transparent gel consisting of 98% water that fills the eyeball between the lens and the retina. It also contains hyaluronic acid, amino acids, soluble proteins, salts, and type II collagen. The vitreous functions to transmit light and contributes a small degree of dioptric power to the eye.

Retina

The retina, forming the internal layer of the eyeball, is where the optical image enters the visual system via phototransduction. The outer layer (adjacent to the choroid) of the retina, composed of the retinal pigmented epithelium (RPE) absorbs light. The inner layer consists of neurosensory cells including rods and cones. At the center of

the posterior part of the retina is the oval, yellowish macula, which is the retinal area that provides for highest visual resolution. One of the biggest drug penetration challenges is the blood-retina-barrier (BRB), which reduces the penetration of systemic drugs targeting the retina. The BRB can be separated into an inner and outer barrier. The tight junctions of the RPE form the outer barrier, restricting paracellular transport of polar solutes across the RPE from the choroid [9]. The inner BRB is due to the tight junctions in the endothelium of retinal vasculature.

Optic Nerve, Optic Disc

The optic nerve consists of the efferent axons of the retina that converge on the optic disc. These unmyelinated fibers run medially through the orbital cavity, into the lateral geniculate nucleus of the brain, and finally relayed to the visual cortex. The optic nerve is surrounded by three meningeal sheaths, which are continuous with those surrounding the brain.

Common Sight-threatening Diseases

Age-related Macular Degeneration

Age-related macular degeneration (AMD) is the leading cause of visual impairment in the United States among individuals over the age of 65 years, affecting more than 1.75 million persons [10, 11]. AMD has two forms - wet and dry – and is caused by excessive aging of the RPE. The wet form of AMD is characterized by choroidal

neovascularization and fluid accumulation in the subretinal space, which often leads to blindness. Dry AMD, the more common form, is associated with drusen formation and RPE atrophy. Drusens are small, yellowish deposits that form within the retina. The slow course of dry AMD leads to scar formation on the retina, which also impairs vision. Wet AMD is often treated with photocoagulation, but there is currently no satisfactory treatment for dry AMD.

Diabetic Retinopathy

Forty percent of diabetic patients in the United States have some degree of diabetic retinopathy [12]. Diabetic retinopathy often leads to neovascularization, proliferative retinopathy (RPE dedifferentiation and proliferation in the vitreous that results in fibrous membrane formation and retinal detachment), and macular edema. Macular edema is swelling of the macula due to subretinal fluid accumulation. Diabetic retinopathy is treated with photocoagulation and vitrectomy, but earlier pharmacologic intervention with antiangiogenics and steroids are under investigation.

Corneal Diseases

The major causes of corneal blindness are corneal scar and active keratitis [13]. Cornea scars often occur as result of keratitis, which includes corneal irritation, inflammation, and infection. Infections on the cornea are caused by bacteria or fungi

following superficial corneal abrasions. Corneal ulcers may also follow trauma, infections of other eye tissues, corneal disorders, and systemic disorders. The only method to restore vision to a scarred cornea is keratoplasty, which have demonstrated high success rates with immunosuppresants.

Chapter 2: Ocular Drug Delivery

Systemic Administration

The systemic route of drug delivery to the eye is subject to the BRB, as it reaches the chorioretinal tissue via the blood circulation [9]. The BRB thus impedes the treatment of many retinal diseases. High and frequent doses of systemically administered medications may be able to penetrate the BRB to provide therapeutic drug levels to the posterior segment; however serious systemic side effects may occur [14]. Therefore, it is important to consider localized drug delivery alternatives, which result in fewer adverse effects.

Topical Administration

Topical ophthalmic drops are the most common method used to administer treatments for ocular disease (Figure 2-1A); however, eye anatomy and physiology pose nearly insurmountable barriers for posterior segment delivery. The two routes for topical delivery to the posterior segment are the corneal and conjunctival/scleral pathways. In both pathways, drug formulations are subject to solution drainage, tear dilution, tear turnover, conjunctival vasculature absorption and the corneal epithelium barrier. An aqueous dose leaves the precorneal area within 5 minutes of instillation in humans and less than 5% of the drug reaches intraocular tissues[9, 15].

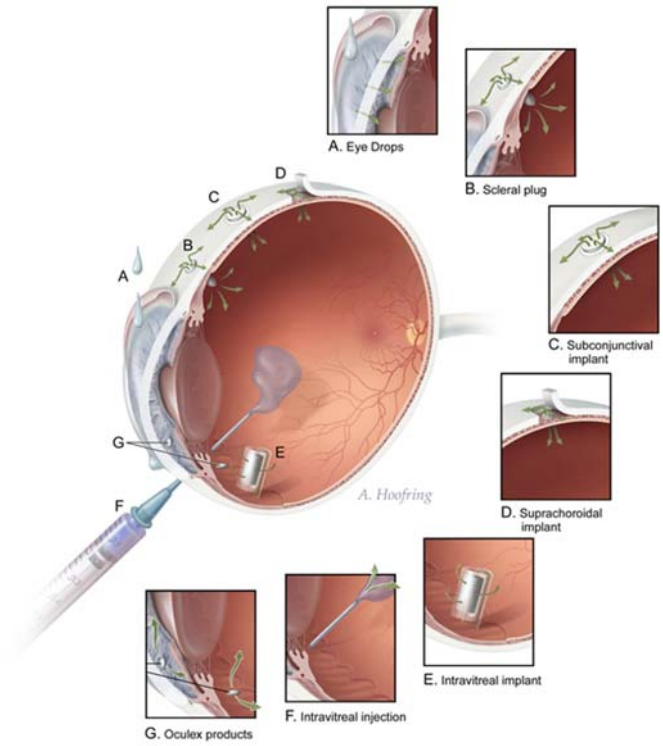

Figure 2-1: Principal methods of local drug delivery to the eye.

Controlled Release Systems

Overview

Controlled release systems, including ocular implants and particulate systems (i.e. microspheres, liposomes), are designed for optimal therapeutic efficacy. These systems should be biocompatible and properly sterilized to minimize the potential for an inflammatory reaction in the eye. In addition, controlled release systems should deliver drug at predictable and constant release rates to achieve therapeutic levels of drug to the target tissue with minimal toxicity to adjacent tissues. It is necessary for systems to be comfortable, preferably visible for inspection in the eye, while avoiding

blockage of the visual axis. Implants should be easily inserted and removed, if not bio-erodible [16] [17]; and must be cost-effective when compared with systemic administration of the same drug. Particulate systems should be small enough to be injected through 20-23 gauge needles [7]. Drug stability is important and needs to be evaluated early during the system development.

Injections

Drug Formulations

Delivery of drugs directly into the eye by intravitreal injection through the pars plana is an approach to achieve therapeutic levels of drug to treat retinal diseases (Figure 2-1F) [18] [19] [20] However, given the short half life of most drugs injected into the vitreous, frequent injections 1–3 times per week are required to maintain therapeutic drug levels. As a result, intravitreal drug injections are very useful in treating acute bacterial infections of the eye that may require one or two injections, but are not well tolerated by patients that may require months or years of injections to treat chronic eye diseases such as age-related macular degeneration or cytomegalovirus- virus (CMV) retinitis, which is a common AIDS manifestation (Figure 2-2). Furthermore, frequent injections increase the risk of retinal detachment, vitreous hemorrhage, endophthalmitis, and cataracts [21] [22] [23].

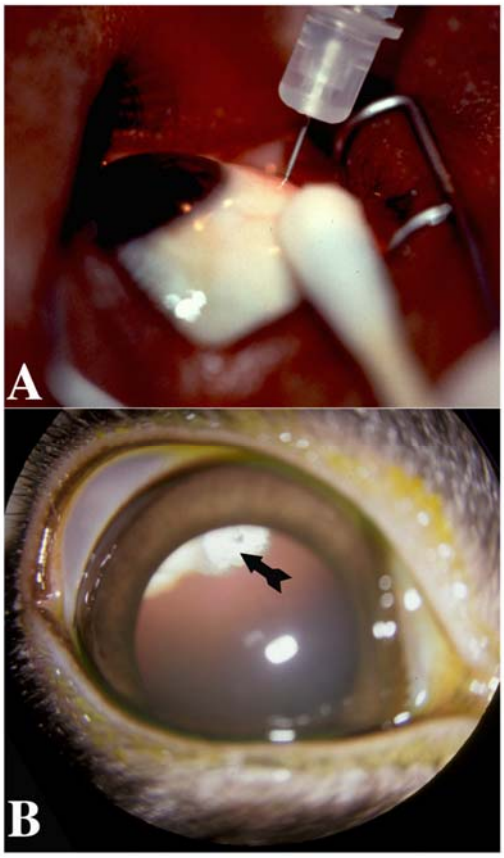

Figure 2-2: A. An external photograph of the eye showing an injection of an anti-viral medication into the vitreous cavity to treat CMV retinitis in a patient with advanced HIV-infection. These injections are repeated twice per week.
B. An external photograph of a rabbit eye showing the front of the eye with the pupil widely dilated. A corticosteroid medication (arrow) had been injected a week before and positioned in the vitreous cavity behind the lens.

A safer alternative to intravitreal injections for drug delivery to the vitreous is the transscleral route achieved with a sub-Tenon's injection. Drug delivery through the sclera in *in vitro* systems shows adequate penetration of corticosteroids [24] and other lipophilic compounds [25]. However, the drug concentrations achieved in the humans vitreous are significantly lower than concentrations achieved by intravitreal injections [26, 27]. Thus, further study is necessary to understand the transscleral clearance mechanisms.

Particulate Systems

Particulate systems that have been investigated for drug delivery to the anterior and posterior segments include micropheres, nanospheres, and liposomes [7, 28] [29-32] [33]. Microspheres and nanospheres are small particle made from biodegradable polymers and drug dispersed either homogenously or amassed at the center. The particles remain at the injection site and release drug through diffusion, chemical reaction, polymer degradation, or ion-exchange mechanisms [34]. Liposomes are small biodegradable vesicles composed of one or more concentric lipid bilayers with aqueous drug at the center. Particulate systems increase the drug retention time and release characteristics can be controlled, achieving higher concentrations in the aqueous or vitreous humor than from the parent drug [7, 34].

Implants

Intraocular implants for drug delivery are capable of bypassing the barriers to intraocular drug absorption and avoid frequent procedures required using intravitreal injection therapy. Drug release rates of implants can be controlled so that therapeutic drug levels are maintained in the eye, while avoiding toxic or subtherapeutic levels. Moreover, higher intraocular drug levels can be achieved using implants compared with systemic or topical administration making the drug more effective for treating a variety of retinal diseases [35]. Since the dose of drug released by intraocular implants is in the range of 0.5 to 10 micrograms per day, these small doses

significantly reduce the risk of systemic drug toxicity. Finally, ocular implants are more convenient for patients and reduces patient compliance issues with taking frequent eye drops or systemic medications [36].

Drug delivery implants can be designed to deliver drug to different parts of the eye (Figure 2-1). The choice of implant design and location in the eye depends on the location of the disease. Since most of the current implants available clinically are diffusion-based, the closer the implant is located to the target tissue, the more drug will be delivered to that site. For example, an implant designed for the subconjunctival space will deliver higher drug concentrations to best treat diseases that affect the conjunctiva or sclera (Figure 2-1 C). Implants designed to directly deliver drug into the vitreous cavity (Figure 2-1 B, D, E, G) are used to treat retinal diseases. The decision to use one implant design over another may also be influenced by the surgical risks of implanting a particular device. For example, implants that require an incision leading to the vitreous cavity significantly increase the risk of vitreous hemorrhage, infection, and retinal detachment. Implants inserted in the subconjunctival space are associated with few complications especially if they are biodegradable and do not require removal. However, implants placed in the subconjunctival space may have some difficultly in treating retinal diseases because the sclera and choroid may pose a formidable obstacle to drug diffusion. Some subconjunctival implants using drugs with high scleral permeability have a reasonable potential to deliver drugs into the eye to treat retinal diseases. Passive solute diffusion through an aqueous pathway is the primary mechanism of drug permeation across the

sclera [15]. In vitro and in vivo flux studies have shown that sclera to be quite permeable to drugs, including monoclonal antibodies, with of a wide range of molecular weights up to 150 kilo Daltons [37] [38, 39]. Transscleral permeability is inversely related to the drug's molecular weight; therefore, small molecule drugs are beneficial when delivering drugs from the subconjunctival space into the eye.

Matrix Implants

The matrix implant design for ocular implants typically consist of uniformly distributed drug in a nonreactive, bioerodible polymer [20] [40]. The most common polymer used is poly (lactic-glycolic acid) (PLGA), which is a copolymer of poly-glycolic acid and poly-lactic acid. PLGA hydrolyzes into organic monomers of lactic acid and glycolic acid and is the same material used for manufacturing absorbable sutures. During the manufacturing process of matrix implants, some of the drug dissolves in the polymeric solution, but the majority remains in solid phase [40]. The relative concentrations of the polymers, such as the lactide:glycolide ratio in PLGA, as well as polymer weight ratios can be altered to adjust the drug release rate [41] [42] [43]. Furthermore, an additional polymer coating and holes in the implants can influence release rates [44]. The polymer coating slows release rates, and larger hole diameters, increases the surface area of release, which correlates with higher release rates. In addition, adjustments of drug release rate are dependent on drug properties. The use of insoluble drugs results in drug release that more closely relates to the dissolution rate of the matrix. Furthermore, the hydrophilicity of the polymer affects the release rate, as more controlled release is exhibited from hydrophobic polymers

[45]. The release of drug from matrix implants follows first-order kinetics i.e. the initial release is robust followed by a rapid decrease in release as the drug in the implant declines [46] [20]. Therefore, matrix style implants are most appropriate for eye conditions with acute onset, such as infectious endophthalmitis or post-operative inflammation, because these conditions are best treated with an initial loading dose of antimicrobials or corticosteroids followed by a gradual tapering of the medications over a defined period of time generally ranging from 1 day to 3 months.

Reservoir Implants

Reservoir implants deliver continuous amounts of drug over months to years, which is desirable for treatment of chronic eye diseases. These devices typically have a central core of drug, coated with a non-reactive polymer [40]. Although polymers used for reservoir implants are generally non-erodible, there are exceptions such as a bio-erodible reservoir ciprofloxacin implant for the treatment of intraocular bacterial infections [20]. Non-erodible silicone, ethylene vinyl acetate (EVA), and polyvinyl alcohol (PVA) are commonly used in reservoir devices. The primary polymers in the first extraocular implant (placed in the inferior conjunctival sac) used for drug delivery were EVA and PVA, developed by Alza Corporation (Mountain View, California) [47, 48] and marketed as the Ocusert® implant. The Ocusert released pilocarpine, a medication used in the treatment of glaucoma, over a 7-day period and was available in 2 different doses. The Ocusert improved patient compliance since pilocarpine eye drops were required every 4 hours to maintain adequate intraocular pressure control.

The application of different polymers to reservoir implants is determined primarily by the permeability of a given drug through the polymer. Silicone and PVA are freely permeable to a number of drugs while providing enough support to hold the drug reservoir together. Silicone, used for the past 3 decades in the manufacture of a 5-year releasing contraceptive implant (Norplant®, Wyeth Pharmaceuticals, Collegeville, Penn.), has been very attractive for use in eye implants because it is biocompatible, inexpensive, easy to handle, and has a long track record of safety in the medical field. PVA, a commonly used polymer in commercial eye drops, can be used in high concentrations (5 to 50%) to coat drug pellets. PVA can be heated up to 200° C to cross-link the polymer, rendering it less soluble to drugs. The duration and temperature of the heat treatment can be varied to control the diffusion of drugs through the PVA. EVA is impermeable to most medications and used as a coating around the drug pellet to provide more controlled diffusion of the drug from the implant. The drug delivery depends on the water that diffuses through the polymer coating and dissolves part of the pellet forming a saturated drug solution. The drug then diffuses back out of the device and as long as the solution inside the device is saturated, the release rate is constant [49]. This mechanism allows the device to deliver a small burst of drug, followed by a steady-state release rate that persists until greater than 90% of the drug pellet has diffused through the polymer. The movement of drug through the polymer in reservoir implants is governed by Fick's Law of Diffusion where the release rate is directly proportional both the surface area of the implant, the diffusivity (i.e. ability of a particular drug to transit through the

polymer), and indirectly proportional to the thickness of the polymeric coating [40]. The most important determinant of the longevity of a reservoir implant is the solubility of the drug in the pellet in the surrounding media. Typically, relatively insoluble drugs will give reservoir implants the longest release rates lasting from 6 months to 5 years. Chronic eye diseases such as AMD and diabetic retinopathy are optimally treated with a constant level of drug release, or zero-order kinetics, delivered using reservoir implants.

The ganciclovir implant was the first intraocular drug delivery implant available for humans and had a profound impact on treatment of CMV retinitis [50]. Clinical trials using the implant were started in 1990 and approval from the FDA occurred in 1996. Marketed under the trade name of Vitrasert® (Bausch and Lomb, Rochester, NY), the implant was constructed by coating a compressed ganciclovir pellet with PVA, which is permeable to the drug, and then partially coated with EVA, which is impermeable to the drug, to reduce the release rate (Figure 2-3). The pellet complex was attached to a PVA suture stub, heated to partially cross-link the PVA and adjust the in vitro release rate to 1.4 microgram/hr. In vivo, the intravitreal drug levels were 4.1 microgram/ml, considerably higher than those levels achieved following intravenous therapy (0.93 microgram/ml) [49, 51]. The device was capable of delivering drug for approximately 8 months. Clinical studies showed that the median time to progression of retinitis in untreated patients (controls) was 15 days, compared with 226 days for patients assigned to immediate treatment with the implant. This compared favorably with reported times to progression in patients treated with intravenous ganciclovir, which was 71 days [52, 53]. Vitrasert implant has emerged as the most efficacious

method of treating CMV retinitis and the patient acceptance is high given the alternatives of frequent biweekly intravitreal injections or daily drug infusions. Because the device eventually runs out of drug and must be replaced, appropriate implant exchange practices have been adopted. The optimal time for exchanging the ganciclovir implant is dictated by the predictability of the duration of release of each device, the location of retinitis, and the overall health of the patient. The duration of release of each implant is dependent on the original quantity of drug, the rate of drug release from the device, and the rate of tissue clearance of the drug [53].

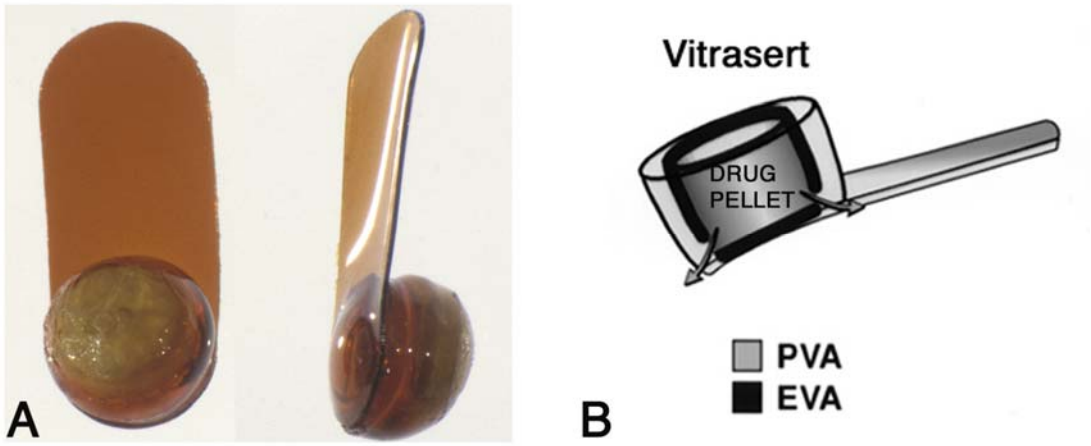

Figure 2-3: A. A Vitrasert implant showing the front and side views. The drug pellet contains ganciclovir, a potent antiviral agent to treat CMV retinitis. The long suture stub is trimmed and used to fixate the implant to the sclera at the pars plana allowing the drug reservoir to release drug into the vitreous cavity. B. A schematic drawing of a Vitrasert implant showing the drug pellet surrounded by 2 polymers, PVA and EVA. Ganciclovir is freely permeable to PVA; however, to reduce the release rate, EVA (not permeable to ganciclovir) coats ~90% of the pellet and drug is released (arrows) at the base of the implant.

Advances in biomedical engineering and surgical techniques have encouraged the development of a variety of intraocular therapeutic devices. Controlled release drug delivery systems have had a profound impact in clinical ophthalmology, especially in

the management of retinal diseases that can lead to blindness. Ocular implants and particulate systems have been engineered to avoid the barriers that often impede the delivery of drug via traditional methods. The investigation and clinical use of ocular drug delivery systems have relied upon an interdisciplinary approach including biomedical engineering and ophthalmology. This team approach is necessary to elucidate ocular barriers and drug clearance mechanisms.

Chapter 3: An In Vivo Model for Assessing the Ocular Barriers to the Transscleral Delivery of Triamcinolone Acetonide

Introduction

Intravitreal corticosteroids have been used for treating retinal diseases; however, complications include vitreous hemorrhage, retinal detachment, and endophthalmitis [54-58]. Transscleral delivery of corticosteroids using sub-Tenon's injections, with drug transport into the vitreous then to the posterior pole, may be a safer alternative to reduce sight-threatening complications [15]. Drug delivery through the sclera with *in vitro* systems show adequate penetration of corticosteroids[24] and other lipophilic compounds [25]. However, recent reports in patients receiving sub-Tenon's triamcinolone acetonide showed marginal results in treating diabetic macular edema[26], especially when compared with direct intravitreal injections [27]. The main barriers to transscleral drug delivery contributing to poor vitreous drug levels are the sclera[37], choroidal vasculature[59], and clearance from conjunctival lymphatics/ blood vessels [60]. Since the relative contribution of each clearance mechanism is not known, they are often combined into one pathway in pharmacokinetic models [6, 60].

To improve our understanding of the *in vivo* clearance mechanisms of corticosteroids, we evaluated vitreous drug levels following sub-Tenon's injection of triamcinolone

acetonide in rabbits with selective elimination of conjunctival lymphatic/blood vessels and the choroid.

Methods

Dutch-belted rabbits of either sex (Covance Laboratories, Inc., Vienna, VA) were used and all procedures adhered to the guidelines from the Association for Research in Vision and Ophthalmology statement for the use of animals in ophthalmic and vision research. Prior to a sub-Tenon's injection of a triamcinolone acetonide formulation or other ophthalmic surgical procedure, animals were anesthetized with ketamine hydrochloride (Fort Dodge, Inc., Fort Dodge, IN; 35mg/kg) IM and xylazine (Phoenix Scientific, Inc., St. Joseph, MO; 5mg/kg) IM; proparacaine 1% ophthalmic drops (Allergan America, Hormigueros, PR) were used topically on the eye. The pupils were dilated with 1 drop each of phenylephrine hydrochloride 2.5% (Akorn, Inc., Decatur, IL) and tropicamide 1% (Alcon, Inc., Humacao, PR). A baseline eye examination including fundoscopy with an indirect ophthalmoscope was performed. Injections were performed in right eye by entering the conjunctiva over the superior rectus area with a 30-gauge hypodermic needle, advancing the needle to the superotemporal quadrant, and injecting sub-Tenon's so the center of depot was 5-6 mm from the limbus (Figure 3-1). The needle was then withdrawn and no drug suspension was observed to leak out of the opening in the conjunctiva. The drug formulation was prepared in a sterile fashion using USP grade triamcinolone acetonide (Voight Global Distribution, LLC, Kansas City, MO) at a 40 mg/ml

concentration by the Clinical Center Pharmacy Department at the National Institutes of Health. The suspending medium was normal saline USP (B. Braun Medical Inc., Irvine, CA) and hydroxypropylmethylcellulose 0.5% USP grade (Dow Chemical Company, Midland, MI). Enucleated eyes were immediately frozen at –80° C to prevent post-mortem drug redistribution.

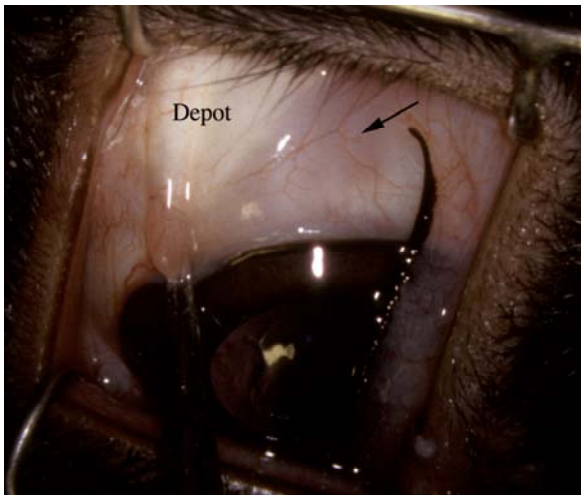

Figure 3-1: An external photograph demonstrating the position of a triamcinolone acetonide depot following a sub-Tenon's injection in the superotemporal quadrant of a rabbit. The hypodermic needle entered the tissue (arrow) medially and was advanced to the superotemporal quadrant before the injection, preventing the back flow of drug.

A total of 6 groups of rabbits were investigated and they had the following procedures:

Group 1: A sub-Tenon's injection of 10-mg of drug was performed, and after 3 hours, the animal was euthanized and the eye enucleated.

Group 2: A sub-Tenon's injection of 20-mg of drug was performed, and after 3 hours, the animal was euthanized and the eye enucleated.

Group 3: The effect of the elimination of both conjunctival and choroidal clearance on transscleral delivery was evaluated in this group. The blood and lymphatic flow that contribute to the conjunctival and choroidal clearance mechanisms was halted in these animals by performing euthanasia immediately following a sub-Tenon's injection of 10-mg of drug. After 3 hours, the right eye was enucleated.

Group 4: To selectively eliminate clearance of drug from the choroidal circulation, cryotherapy was performed in the superotemporal quadrant to obliterate the choroidal blood flow. The effects of cryotherapy on ocular tissues have been well described in the literature. Following a single freeze/thaw cycle with cryotherapy, histology studies demonstrate sloughing of the superficial conjunctival epithelium and the Tenon's fascia is spared [61]. The Tenon's fascia provides a scaffold for the rapid re-epithelialization from the surrounding untreated conjunctival epithelium[61]. To irreversibly damage Tenon's fascia with cryotherapy, as in the case of eradicating conjunctival tumors, multiple freeze/ thaw cycles are required and Tenon's fascia becomes fibrotic [61-63]. The sclera is also resistant to cryotherapy. Scleral edema present histologically resolves after 3-days[64] and there are no alterations in drug permeability or ultrastructure of the sclera by electron microscopy [65]. Although there are no reported permanent alterations in the conjunctival and scleral tissues, the intraocular tissues, namely the ciliary body[66] and choroid/retina[64], are very sensitive to single freeze/thaw cryotherapy applications and the tissues undergo ischemic necrosis [62]. Within 1 to 4 weeks following cryotherapy, there is clinical evidence of a chorioretinal scar [67]. Histology studies show the choroid and retina

are replaced with a glial scar and the choriocapillaris and retinal vasculature are obliterated with rare large choroidal vessels remaining patent [64, 67-69]. The cryotherapy in the present study was performed using a single freeze/thaw cycle to preserve the conjunctiva and sclera and produce a chorioretinal scar. The cryotherapy was performed under direct visualization to produce visible whitening of the choroid and retina at a temperature of –60° C with a 2.5 mm retinal probe attached to Keeler CTU CO_2 Cryo Unit (Keeler Instruments, Broomall, PA). A total of 8 adjacent cryotherapy applications in 2 horizontal rows were placed in the superotemporal quadrant of the right eye with the anterior edge 4 mm from the limbus. Fundus examinations were performed using indirect ophthalmoscopy over a minimum of 1-month to ensure that a mature chorioretinal scar formed between the medullary ray and ora serrata (Figure 3-2). After a mature chorioretinal scar formed, rabbits in this group received a sub-Tenon's injection of 10-mg of drug, and after 3 hours, the animal was euthanized and the eye enucleated.

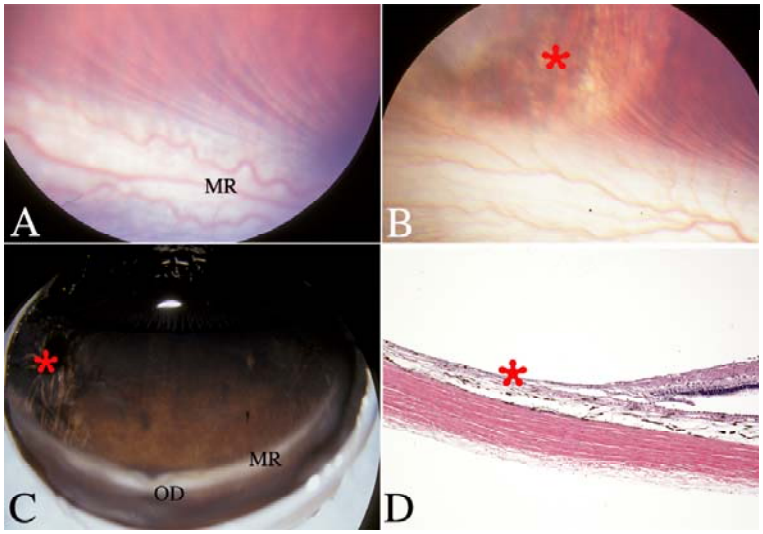

Figure 3-2: A. A photograph of a normal rabbit fundus (right eye) showing the temporal medullary ray (MR) and normal retina above. (original magnification, 1.5x). B. A retinal photograph of the rabbit eye in figure 2A, 1-week post-cryotherapy showing the typical pigmentary changes (red asterisk) over the medullary ray. (original magnification, 1.5x). C. The enucleated rabbit eye shown in figure 2B was bisected showing the chorioretinal scar (red asterisk) 4-weeks following cryotherapy. OD optic disc, MR medullary ray. D. Photomicrograph showing the border between normal retina/choroid and a chorioretinal scar (red asterisk) in the eye shown in figure 2C. Large choroidal vessels were present in some sections (stain, hematoxylin and eosin, original magnification, x200).

Group 5: To selectively inhibit the clearance from conjunctival lymphatic/blood vessels, we first reviewed the literature on the anatomy of the eye in this region. The lymphatic vessels in the conjunctiva are one of the most extensive lymphatic network described in any organ system in the body[70] and occur in a superficial and deep plexus within Tenon's fascia (Figure 3-3) [70-73], similar to the distribution pattern observed in skin [70]. Blood vessels are distributed throughout the Tenon's fascia and venous drainage vessels are more numerous than the arteries [74]. In humans, there is a concentration of blood vessels in the episcleral region[74] that is lacking in rabbits [75, 76]. To inhibit the clearance of a sub-Tenon's injection of triamcinolone acetonide, a 'conjunctival window' was created by incising an 7 mm x 7 mm x 7 mm square through the conjunctiva in the superotemporal quadrant of the right eye down to bare sclera using Wescott scissors and toothed forceps. The conjunctiva remained attached at the cornea and the posterior corners to keep the tissues taut and flat against the sclera (Figure 3-4). A sub-Tenon's injection of 10-mg of drug was performed with the depot centered within the 'conjunctival window.' After 3 hours, the right eye was enucleated.

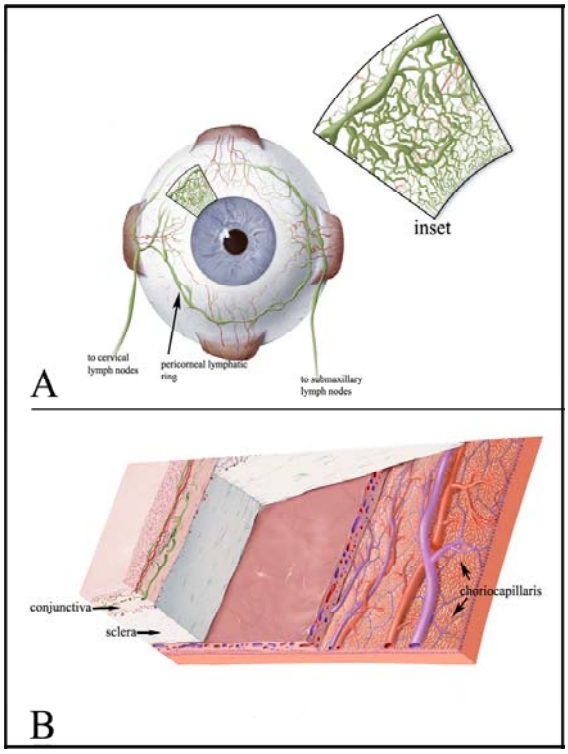

Figure 3-3: A. A schematic drawing showing the distribution of lymph (green) and blood vessels in the conjunctiva. A circular lymphatic trunk termed the 'pericorneal lymphatic ring,' is a centralized collection channel that drains medially and temporally to regional lymph nodes. Inset: a magnified area at the limbus demonstrating the dense plexus of lymphatic vessels in the conjunctiva. B. A schematic drawing of the cross section of an eye near the equator highlighting the main ocular barriers to transscleral drug delivery. Lymphatic vessels in the conjunctiva occur as a superficial plexus immediately beneath the epithelium and a deeper plexus with larger lumen structures within the Tenon's fascia. Blood vessels are distributed throughout the Tenon's fascia, and in humans, there is a concentration of blood vessels in the episcleral region.

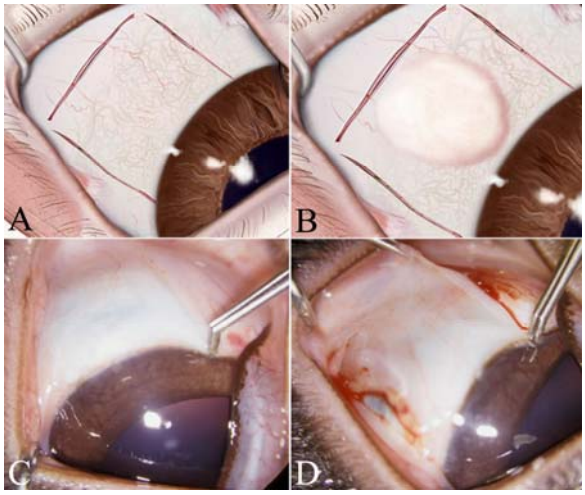

Figure 3-4: (A) An illustration of a 'conjunctival window' in the superotemporal quadrant of a rabbit eye demonstrating the full-thickness incisions through conjunctiva to bare sclera. Attachments remain intact at the limbus and the 2 posterior corners to keep the tissues flat against the sclera. (B) An illustration of a triamcinolone acetonide depot following an injection in the sub-Tenon's space of a 'conjunctival window.' (C) An external photograph of the superotemporal quadrant of a rabbit eye showing normal tissues. (D)An external photograph of the superotemporal quadrant of a rabbit eye demonstrating the full-thickness radial incisions through the conjunctiva to bare sclera. The superior radial incision follows the temporal border of the superior rectus muscle. Following the radial incisions, the eye was rotated down, and with the conjunctiva taught against the sclera, the posterior incision was performed.

Group 6: To determine whether the chorioretinal scar following cryotherapy inhibited the transit of drug into the vitreous, a sub-Tenon's injection of 10-mg of drug was performed in animals that received previous cryotherapy. Following the

injection, the animal was immediately euthanized, and after 3 hours, the right eye was enucleated.

In all groups, euthanasia was performed with an intracardiac pentobarbital overdose (Beuthanasia-D Special, Schering-Plough Animal Health Corp., Kenilworth, NJ). The eyes were dissected while frozen and the vitreous humor isolated using previously described methods [77]. The triamcinolone acetonide was extracted by placing the vitreous in HPLC grade acetonitrile (Fisher Scientific, Pittsburgh, PA) in sealed vials for 24 hours at room temperature, sonicated using a GEX 600 Ultrasonic processor (Daigger, Lincolnshire, Il) for 60 seconds, and stored in sealed vials for another 24 hours at room temperature. The samples were spun down in a Centra C12 centrifuge (Thermo IEC, Needham Heights, MA) for 3 minutes at 3,500 rpm and the supernatants were submitted for HPLC analysis. The drug assays were performed using an Agilent HP1100 HPLC system (Agilent Technologies, Palo Alto, CA) equipped with a G1329A autosampler, a G1315A diode array detector, a G1312A binary pump, and a Dell workstation which controlled the operation of HPLC and analyzed the data. A Beckman Ultrasphere C-18 column (5 μm, 4.6x250 mm)(Beckman Coulter, Inc., Fullerton, CA) was used for separation, and detection was set at 254 nm. The flow rate employed was 1.0 ml/min with a mobile phase of 60% of acetonitrile and 40% of water by volume. The retention time was 7.0 min and detection limit was 10 ng/ml. The vitreous concentrations were recorded for each rabbit in each group in microgram/ milliter (μg/ml).

Results

A total of 20 rabbits were used in the 6 rabbit groups and the vitreous concentrations of triamcinolone acetonide were recorded in Table 3-1. There were no detectable drug levels in groups 1 and 4 in all rabbits. The data for the other groups showed considerable variability in results between rabbits in some of the groups; therefore, statistically testing the concentration differences between groups was not performed. In Group 5 rabbits, one may argue that the vitreous drug levels recorded were not from transscleral delivery but from diffusion of the drug from the cut edges of the 'conjunctival window' through the anterior chamber into the vitreous. Therefore, the last 3 rabbits evaluated in this group had aqueous humor drug levels measured and they were undetectable in all animals. This suggested that the drug entered the vitreous cavity from the sub-Tenon's space through a transscleral route.

Table 3-1

Vitreous concentrations of Triamcinolone Acetonide in Rabbit Groups

Group number	Vitreous drug level μg ml^{-1} (mean±S.D.)
Group 1 ($n=3$) 10-mg injection	Not detected
Group 2 ($n=3$) 20-mg injection	16.56±16.44
Group 3 ($n=3$) 10-mg injection with immediate euthanasia	7.13±1.94
Group 4 ($n=3$) choroidal clearance elimination with cryotherapy, 10-mg injection	Not detected
Group 5 ($n=5$) conjunctival lymphatic/blood vessel elimination with 'conjunctival window', 10-mg injection	7.36±6.45
Group 6 ($n=3$) choroidal clearance elimination with cryotherapy, 10-mg injection with immediate euthanasia	12.76±11.62

Discussion

There are a number of important observations that are apparent from the results of this *in vivo* model. Live rabbits (Group 1) had no detectable vitreous drug concentration following a 10-mg sub-Tenon's injection of triamcinolone acetonide. However, in Group 3, where the animals were immediately euthanized, effectively terminating the clearance from conjunctival lymphatic/blood vessels and the choroid, drug was present in the vitreous. This suggested that the tissues themselves (i.e. sclera, non-perfused choroid and retina) may not be the primary barrier to drug transport into the eye, and other factors present *in vivo,* such as lymph and blood transport, may play an inhibitory role in transscleral drug delivery to the vitreous. Rapid transscleral movement into the vitreous when lymph and blood clearance had been halted following euthanasia was recently demonstrated by using hydrophilic contrast agents and magnetic resonance imaging (MRI) (Figure 5A & B) [78]. It appears that both hydrophilic, and lipophilic drugs as shown in the present study, can transit through tissues when lymph and blood clearance has been terminated. Studies are in progress with our *in vivo* model to specifically examine the relative effects of transscleral delivery as a function of a drug's molecular weight, molecular radius, and drug solubility.

There were drug levels in the vitreous when a 20-mg depot of triamcinolone acetonide was injected in the sub-Tenon's space in live rabbits (Group 2), in contrast to the 10-mg depot from Group 1 that produced no detectable vitreous levels. It had been previously shown in other models that the release of drug from triamcinolone acetonide depots were higher with larger weight depots [79]. Extrapolating from an ocular pharmacokinetic model developed for triamcinolone acetonide depots[80], over a 3-hour period, the 10-mg depot was estimated to release at a mean of 8 microgram per hour; the 20-mg depot released at a mean of 13 microgram per hour. Since a 10-mg depot was not able to deliver drug into the vitreous in the present study, and the 20-mg depot was successful, one can estimate that the clearance rate of triamcinolone acetonide from the sub-Tenon's space is between 8 microgram per hour and 13 microgram per hour. Drug depots, with release rates that exceed the tissue clearance rates, will deliver drug into the vitreous. Estimating these parameters is important when developing sustained-release devices for placement in the sub-Tenon's space to deliver drug to the vitreous. Since the typical release rate of a corticosteroid-eluting implant manufactured for vitreous insertion is < 0.125 microgram per hour[81], substantially higher drug release rates would be required from sub-Tenon's implants to bypass the transscleral drug transport barriers in order to deliver drug to the vitreous. These data are consistent with human studies where small depots (e.g. 5-mg or less of triamcinolone acetonide) were injected in the sub-Tenon's space and the majority of patients had no recordable vitreous drug levels a median of 5.5 days after the injection[82], whereas patients injected with 40-mg depots had detectable vitreous drug levels at 4-weeks [83]. Animal studies using

depot-corticosteroid preparations showed that vitreous drug levels following subconjunctival or sub-Tenon's injection were highest within the first 24 to 72 hours after the injection and rapidly tapered off over 1- to 2-weeks [84, 85]. An explanation for this rapid reduction in vitreous drug concentrations is that the depot becomes smaller with time and the drug release rate from the depot falls below the threshold required to overcome the clearance mechanisms. This results in poorly sustained vitreous drug concentrations which may account for the limited efficacy when using sub-Tenon's triamcinolone acetonide injections for diabetic macular edema [26, 27].

Although vitreous drug levels were undetectable 2-weeks following a 40-mg anterior or posterior sub-Tenon's triamcinolone acetonide injection in rabbits, aqueous humor levels were detectable for at least 2-months following injections (Robinson et al. Unpublished data). Aqueous humor drug levels may have been sustained following sub-Tenon's injections by drug entrance through the ciliary body area. This 'portal of entry' zone in the ciliary body was described separately by 2 groups with MRI in live rabbits using contrast agents in the sub-Tenon's space [59, 60]. Unfortunately, the prolonged anterior segment exposure to corticosteroids can lead to ocular hypertension appearing as late as 6-months following the injection in patients with retained drug depots in the sub-Tenon's space [86].

Although it is generally accepted that the choriocapillaris is involved with clearing compounds following an intravitreal injection[60, 87-89], the elimination of the choroid in this study utilizing cryotherapy (Group 4 rabbits) did not produce the

vitreous drug concentrations following a sub-Tenon's triamcinolone acetonide injection. A possible explanation was that the release rate from the drug depot did not exceed the clearance rate from the conjunctival lymphatics/blood vessels and the absence of the choroid was not relevant. It was unlikely that the chorioretinal scar itself impeded drug transport since drug was still able to transit through the scar into the vitreous in euthanized animals (Group 6 rabbits). Surprisingly, the elimination of the conjunctival lymphatics/blood vessels (Group 5 rabbits), with an intact choroid, allowed the transit of drug into the vitreous. This suggested that the conjunctival clearance pathways were possibly more effective than drug clearance via the choroidal vasculature to inhibit triamcinolone acetonide transport into the vitreous in this rabbit model.

The transport of compounds in the blood and lymph have been well studied in other organ systems [90]. Once thought to be primarily involved with the transport of macromolecules[91], the lymphatics are important for the transport of different molecular weight compounds and drugs[92-95], especially small molecular weight lipophilic compounds like corticosteroids [90]. Although our experiment did not distinguish between clearance of triamcinolone acetonide from the sub-Tenon's space via conjunctival lymphatics or conjunctival blood vessels, we have previously demonstrated that a similar molecular weight drug was transported into the ipsilateral cervical lymph nodes within 1-hour after placement of an episcleral sustained-release implant [89, 96, 97]. Investigators examining the drug concentrations in the ipsilateral cervical lymph nodes have shown significant lymphatic clearance from the sub-

Tenon's space of small molecular weight hydrophilic compounds such as gadolinium-DTPA[60], and compounds as large as albumin [98-100]. Further studies applying lymphatic diversion/ligation techniques [101, 102] used to investigate the afferent lymphatic drainage of the brain through the cervical lymph nodes may be necessary to determine the relative contributions of the lymph and blood in drug elimination from the eye.

Transscleral drug delivery has classically been studied with *in vitro* methods using perfusion apparatuses with isolated sclera ± choroid tissue mounted between two chambers [24, 25, 38, 39, 65, 103, 104]. Since the results of this study suggested that the conjunctival lymphatic/blood vessels in the live animal may be a factor in the clearance of drugs from the sub-Tenon's space, *in vivo* models may be a more clinically relevant approach in studying the transscleral delivery of drugs. Furthermore, when establishing *in vivo* models to study transscleral drug delivery, one must be cognizant of the clearance role of the conjunctival lymphatic/blood vessels. For example, delivering a drug under a partial thickness scleral flap [38, 39] may bypass the conjunctival elimination pathways and yield different vitreous drug concentrations compared with a delivery system that releases into Tenon's fascia.

Although the rabbit is a commonly used animal in ocular pharmacology, there are differences in the anatomy of the rabbit eye that have to be considered when extrapolating the results of this study to humans [105, 106]. Compared with humans, the rabbit has a lower mean scleral thickness[105], higher choroidal flow rates[107,

108], a smaller vitreous volume[105], and a poorly vascularized retina [106]. Nevertheless, from the viewpoint of transscleral transport studies, the permeability of the sclera is similar in both species using a number of different compounds [38, 39]. Furthermore, the anatomy and physiology of the lymphatic system is similar to the human establishing the rabbit as a common species for lymphatic studies of other organ systems [90, 101].

In summary, the rabbit appeared to demonstrate saturable ocular barriers to transscleral delivery of triamcinolone acetonide into the vitreous following a sub-Tenon's injection. The results suggested that the conjunctival lymphatics/ blood vessels may be a predominant barrier to the delivery of triamcinolone acetonide to the vitreous in this rabbit model. The barrier location and clearance abilities of the ocular tissues are important to consider when developing a successful transscleral drug delivery system. *In vivo* models, retaining the dynamics of blood and lymph flow, may improve the basic understanding of the ocular barriers involved with transscleral drug transport.

Chapter 4: The Pharmacokinetics and Toxicity of a Novel Episcleral Cyclosporine Implant for High-Risk Keratoplasties

Introduction

Penetrating keratoplasties (PKP) are one of the most common and successful allografts performed in the United States. However, high-risk PKPs, where patients have vascularized corneas, have rejection rates greater than 65% [109]and can have corneal graft failure in over 50% of cases within the first year [110] [111]. Cyclosporine (CsA), an immunosuppressive drug used to prevent allograft rejection [112], has demonstrated some efficacy in prolonging high-risk PKPs in humans[113] following systemic administration; however, adverse side effects such as nephrotoxicity and hypertension limits its long-term use in some patients [114, 115]. The use of topical CsA is also limited by poor penetration of the corneal and conjunctival epithelium which leads to subtherapeutic drug levels to prevent allograft rejection [116-121]. As a result, sustained-release implants delivering CsA to the cornea have been investigated and have shown some success in preventing graft rejection in high-risk experimental models [122]. We previously reported the success in delivering therapeutic drug concentrations to the lacrimal gland with a sustained-release CsA episcleral implant [89]. Consequently, we examined a similar implant to see if a single device could deliver therapeutic drug levels throughout the entire cornea, and how rapidly therapeutic drug levels could be achieved. In addition, we report the results of a 1-year pharmacokinetic and toxicity evaluation of the implant.

Materials and Methods

Implant Manufacturing

We developed an implant with a release rate profile based on the typical immunosuppression therapy for prevention of corneal allograft rejection, starting with a high dose followed by a tapering maintenance dose [111]. The goal was to deliver cyclosporine to the cornea for 12 months from a silicone-based matrix-style implant release system[123], using previously described methods of implant preparation [124] [89]. In summary, the implants were made in a polytetrafluoroethylene mold with impressions on the surface measuring 0.75 inch long or 0.50 inch long, 0.08 inch wide, and 0.04 inch in height (width was measured on the flat side; height was measure from the flat surface to the bottom of the rounded depression)(Figure 4-1). The flat side of the implant was the posterior surface, which was applied to the episclera, and the rounded side was the anterior surface. Cyclosporine powder (Xenos Bioresources, Inc., Santa Barbara, CA) was thoroughly mixed with medical grade silicone with a platinum cure system (Nusil Technology, Carpinteria, CA) so that the weight of the drug as a percentage of the total weight of the implant (wt/wt) was 30%. The impressions were filled with the cyclosporine-silicone paste using a metal spatula and cured for a minimum of 24 hours at room temperature. The implants were sterilized with gamma irradiation (25-30 kGy).

Figure 4-1: An episcleral implant measuring 0.75 inch long or 0.50 inch long, 0.08 inch wide, and 0.04 inch in height. Width was measured on the flat side; height was measure from the flat surface to top of the rounded surface.

In Vitro Release Rate

In vitro release rate determination was continued from our previously reported experiment[89] to study 1 year pharmacokinetics of the CsA implants. Representative implants of each length were weighed and placed in individual glass scintillation vials with 10 mL of phosphate buffered saline (PBS) (pH 7.4). Each vial was placed in a shaking water bath at 37°C, and the PBS in each vial was replaced every 24 hours, 5 days a week. In vitro release rates from the implants were determined by assaying the cyclosporine concentrations in the vial over time with a reversed-phase high-performance liquid chromatography (HPLC) assay. Samples or standards with volumes of 5 to 200 μL were injected with an autosampler (model

G1329A; Agilent Technologies, Palo Alto, CA). A 250 x 4.6-mm (5-mm) C18 polymeric column (Vydac, Hesperia, CA) was heated to 80°C in a column heater (model G1316Al; Agilent). Separation was conducted by 1 mL/min isocratic elution with an acetonitrile/water/methanol/*o*- phosphoric acid (600:325:75:0.5) mobile phase and a pump (model G1312A; Agilent). The concentrations of the samples were monitored at 210 nm with an ultraviolet (UV) detector (model G115A; Aglient) and analyzed with Chemstation software, Agilent. The standard curve was linear (r^2 = 1.000) over the range of 46 to 23,360 ng/mL, and the deviation between replicate samples was <5%. The drug detection limit for cyclosporine in solvent was 0.01 µg/mL. The cumulative release of drug from the implants was determined by calculating the area under the release rate curve with the trapezoidal rule and recording it in milligrams ± 1 standard deviation (SD). Sampling time points were daily for the first 2 weeks (for 5 days a week), twice weekly for 1 month, and weekly thereafter for 1 year.

Ocular Pharmacokinetics

Short-term Pharmacokinetics

New Zealand White (NZW) rabbits of either sex weighing 2-3 kg (Covance Laboratories, Inc., Vienna, VA) were anesthetized with ketamine hydrochloride (Fort Dodge, Inc., Fort Dodge, IN; 35mg/kg) IM and xylazine (Phoenix Scientific, Inc., St. Joseph, MO; 5mg/kg) IM; proparacaine 1% ophthalmic drops (Allergan America, Hormigueros, PR) were used topically on the right eye. The pupils were dilated with

1 drop each of phenylephrine hydrochloride 2.5% (Akorn, Inc., Decatur, IL) and tropicamide 1% (Alcon, Inc., Humacao, PR). A baseline eye examination including fundoscopy with an indirect ophthalmoscope was performed. A toothed forceps was used to lift the conjunctiva and Tenon's fascia in the superotemporal quadrant and a 3-mm incision was made with a Wescott tenotomy scissors. A pocket was formed in the sub-Tenon's space and a 0.50 inch cyclosporine implant was placed on the episclera, 5 mm posterior and parallel to the limbus in one eye. No sutures were used to secure the implants. The conjunctiva and Tenon's fascia were reapproximated with a single 9-0 vicryl suture. Bacitracin ophthalmic ointment was placed in the operative eye following surgery. Animals were euthanized at 3 and 72 hours post-implantation with an intracardiac pentobarbital overdose (Beuthanasia-D Special, Scheming-Plough Animal Health Corp., Kenilworth, NJ). Animals were also euthanized at 1 hour and 1 week to determine CsA concentrations in the buccal lymph node. Following euthanasia, the implanted eye was enucleated and 5 mm x 5 mm sections of bulbar conjunctiva adjacent to the limbus were removed superiorly, nasally, inferiorly, and temporally, to examine the relative difference in cyclosporine concentrations around the eye. The globes were immediately frozen at –70˚C for later dissection and drug extraction. The time from enucleation to freezing was rapid (<10 seconds) which limited postmortem drug redistribution. The eyes were dissected while frozen and circular sections of sclera, were removed superiorly, nasally, inferiorly, and temporally with a 6-mm diameter trephine, centered 5 mm away from the limbus. Three contiguous circular sections of cornea were also removed with a 6-mm diameter trephine with the center of the sections 8, 13, and 18

mm away from the center of the implant to study the rate and amount of cyclosporine distribution at various distances from the implant. (Figure 4-2) The frozen globe was then cut 360 degrees around at the limbus with a razor blade and the remainder of the cornea lifted cleanly off of the frozen aqueous humor. A razor blade was passed parallel to the front surface of the iris, and the frozen aqueous humor lifted off the iris/lens diaphragm in 2 to 3 frozen pieces. Other ocular tissues isolated for drug analysis included the vitreous humor, and residual scleral and conjunctival body. In addition, lacrimal gland tissue was extracted at 1 hour and 1 week. Cyclosporine was extracted by placing the ocular tissues in HPLC grade acetonitrile (Fisher Scientific, Pittsburgh, PA) in sealed vials for 24 hours at room temperature, sonicated using a GEX 600 Ultrasonic processor, (Daigger, Lincolnshire, Il) for 60 seconds, and stored in sealed vials for another 24 hours at room temperature. The samples were spun down in a Centra C12 centrifuge (Thermo IEC, Needham Heights, MA) for 30 minutes at 3,500 rpm and the supernatants were submitted for HPLC analysis. The cyclosporine concentrations were expressed as microgram/milligram (μg/mg) of tissue.

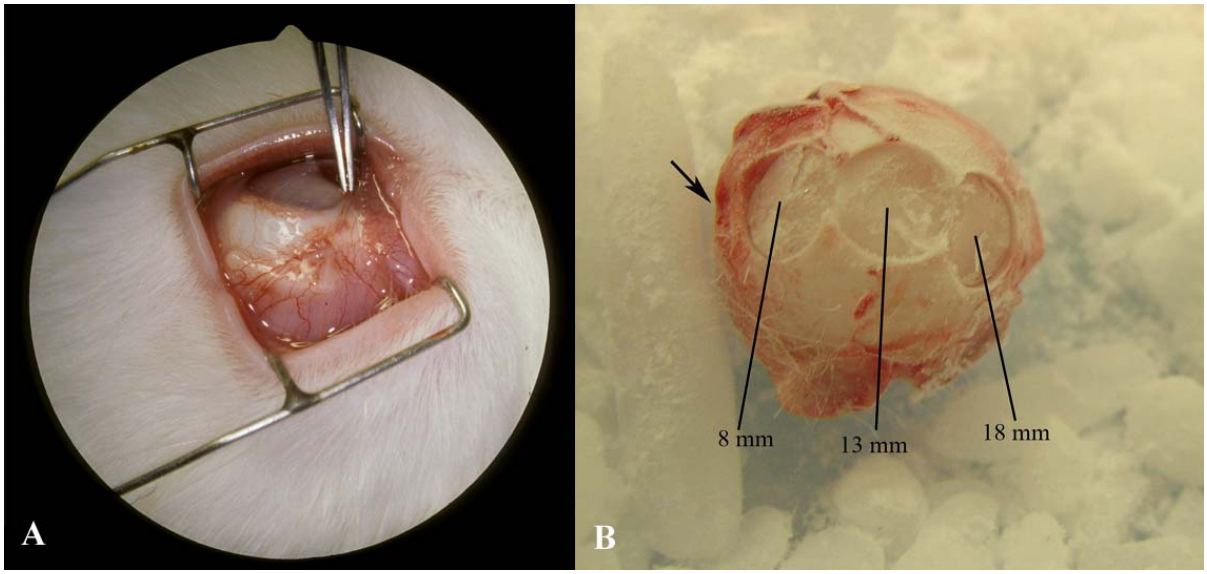

Figure 4-2: Placement of episcleral cyclosporine implant (*A*) superotemporally 5 mm from limbus. Circular sections (*B*) of the cornea are removed to measure the drug concentration at different regions. Distances are measured from the implant (*arrow*) which is superotemporal.

Long-term Pharmacokinetics

We extended the previously reported study[89] of the cyclosporine distribution in the ocular tissues over time following implant surgery in normal research beagles. Using methods previously described, the 0.75 inch implant was placed superotemporally in one eye 5 mm from the limbus, and the animals were sacrificed at 1, 3, 6, 9, and 12 months subsequent to implantation. Ocular tissues, including the cornea, conjunctiva, sclera, lacrimal gland, third-eyelid gland, lens, ciliary body, aqueous humor, vitreous humor, upper and lower eyelid tarsus, and tarsal conjunctiva were separated for drug extraction using the methods described above.

Toxicity Evaluation

A toxicology study was performed using the 0.75 inch implant and 1 device was inserted into one eye of each dog. The ocular toxicity was evaluated by clinical examination, serial electroretinography, and histopathology. All procedures adhered to the guidelines from the Association for Research in Vision and Ophthalmology statement for the use of animals in ophthalmic and vision research.

Normal research beagles (Marshall Farms, Inc., North Rose, NY) were anesthetized with acepromazine (Abbott Laboratories, Chicago, IL; 0.02 mg/kg) IM and hydromorphone HCl injection (Abbott Laboratories, Chicago, IL; 0.11 mg/kg) IM. Proparacaine 1% ophthalmic drops (Allergan America, Hormigueros, PR) were used topically on the eye. The pupils were dilated with 1 drop each of phenylephrine hydrochloride 2.5% (Akorn, Inc., Decatur, IL) and tropicamide 1% (Alcon, Inc., Humacao, PR). A baseline eye examination including fundoscopy with an indirect ophthalmoscope and intraocular pressure measurement was performed. The conjunctiva and Tenon's fascia in the superotemporal quadrant were lifted with a toothed forceps and a 3-mm incision was made with a Wescott tenotomy scissors. A pocket was formed in the sub-Tenon's space and a 0.75" device was placed on the episclera, 5 millimeters posterior and parallel to the limbus in one eye. No sutures were used to secure the implant to the sclera and a 6-0 vicryl suture was used to close the conjunctival incision. Bacitracin ophthalmic ointment was placed in the operative eye twice daily for 3 days. Following the implant surgery, clinical eye examinations

including a Schirmer's tear test, laboratory work (serum chemistries, renal and liver function tests, complete blood count), and electroretinogram (ERG) recordings were performed over a 12-month period in awake animals. The ERG measures the mass retinal response to a stimulus of light using electrodes placed at the cornea and on the skin around the eye. A flash of light is shown to the rabbit and the electrodes record the retinal potentials which develop as a response to the flash. ERGs were recorded from each eye separately after 5 minutes of dark adaptation. A monopolar contact lens electrode (ERG-jet, La Chaux des Fonds, Switzerland) was placed on the cornea and served as the active electrode. A Barraquer eyelid speculum connected to an electrode wire served as the indifferent electrode, and a subdermal needle electrode inserted in the forehead area as the ground electrode. ERGs were elicited by brief flashes at 0.33 Hz delivered with a Grass PS22 photostimulator (Grass Instruments, Quincy, MA) at maximal intensity, coupled to an 18-inch long optic guide of 0.5 inch diameter. Responses were amplified, filtered, and averaged with a Nicolet Spirit signal averager (Nicolet Instruments Corp., Madison, WI). Averages of 10 responses were measured to obtain peak amplitude values of a-waves and b-waves. The a-wave reflects the general physiological health of the photoreceptors in the outer retina, and the b-wave reflects the health of the inner layers of the retina, including the ON bipolar cells and the Muller cells [125]. Recordings were performed at baseline, 6 months, and 12 months. Differences in the mean amplitudes at each recording were compared with the baseline (pre-implant) values for each eye and tested by the analysis of variance (ANOVA) using PSI-Plot version 7.0 (Poly Software International, Inc., Pearl River, NY). Differences were considered likely to be

clinically significant if the P-value was ≤ 0.05. Animals were euthanized at 12 months, all the eyes were enucleated, and submitted for histopathology. The subgroup of animals used for histological evaluation were anesthetized and then euthanized with an intracardiac pentobarbital overdose (Beuthanasia-D Special, Schering-Plough Animal Health Corp., Kenilworth, NJ). Both eyes were enucleated leaving the implants and overlying conjunctiva intact. All tissues were placed in 10% formalin for a minimum of 7 days. The globes were sectioned perpendicular to the long axis of the implants and through the optic discs. All tissue specimens were placed in increasing concentrations of ethanol, cleared with xylene using a Jung Histokinette Tissue Processor (Leica, Inc., Deerfield, Il), and embedded in paraffin using a Shandon Embedding Center (Shandon, Inc, Pittsburgh, PA). Sections of 7 μm thickness were obtained using a microkeratome, stained with hematoxylin and eosin and representative slide mounted sections were examined by light microscopy.

Statistical Analysis

Statistical analysis was performed using the resampling test and statistical significance was assigned to $p \leq 0.05$.

Results

In Vitro Release Rate

In vitro release rates were continued on 5 randomly selected implants from each lot of 0.75 inch and 0.5 inch, and total mean weights were 40.6 ± 1.8 mg and 25.8 ± 1.6 mg, respectively, and the amount of CsA initially loaded into the implants was 12.18 and 7.74 mg [89]. The *in vitro* release pattern of all implants was typical of a matrix implant whose release kinetics is governed by diffusion from dispersed drug in a polymer (Figure 4-3) [126]. The release rate from 150 days to 400 days (approximately 5 months to 1 year) was sustained, and the final cumulative release for the 0.75 inch and 0.5 inch implants was 3.8 ± 0.3 mg and 2.3 ± 0.3 mg, which was approximately 30% of the initial drug loading.

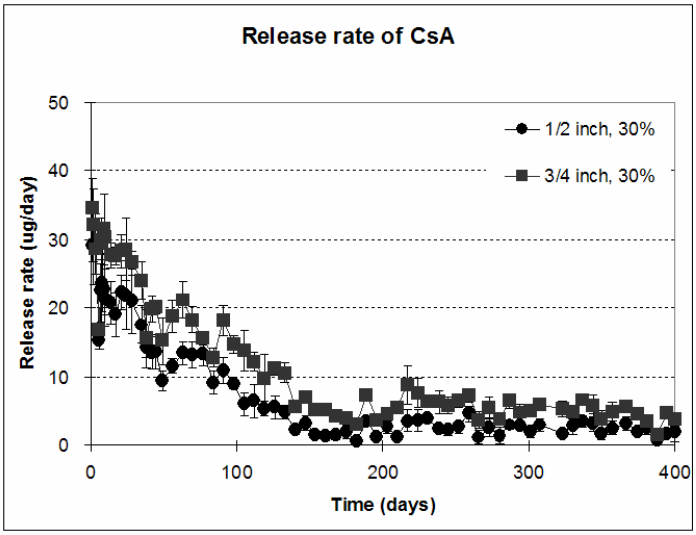

Figure 4-3: *In vitro* release rates of cyclosporine episcleral implant shows sustained-release typical of matrix implants with drug dispersed in polymer.

Short-term Pharmacokinetics

Twelve NZW rabbits received 0.5-inch episcleral implants superotemporally and 5 mm posterior to the limbus. Drug extraction was performed on the right eye of 3 rabbits at each time point studied. Three hours after implantation, the cornea had CsA concentrations of 0.15 ± 0.06 ug/mg, 0.07 ± 0.02 ug/mg, and 0.05 ± 0.02 ug/mg at 8, 13, and 18 mm away from the implant site (Figure 4-4). 72 hours after implant placement, the corneal CsA concentrations were 0.10 ± 0.06 ug/mg, 0.09 ± 0.03 ug/mg, and 0.05 ± 0.03 ug/mg at 8, 13, and 18 mm away from the implant site. The concentration of the superior and inferior conjunctiva at 3 hours was 0.11 ± 0.03 ug/mg and 0.04 ± 0.01 ug/mg, respectively (Figure 4-5). At 72 hours, the superior and inferior conjunctiva concentrations were 0.13 ± 0.06 ug/mg and 0.13 ± 0.03 ug/mg. Drug extraction was also performed on the draining buccal lymph node of 3 rabbits at each time point. The lymph node concentration of CsA was 0.10 ± 0.04 ug/mg and 0.06 ± 0.02 ug/mg at 1 hour and 1 week respectively.

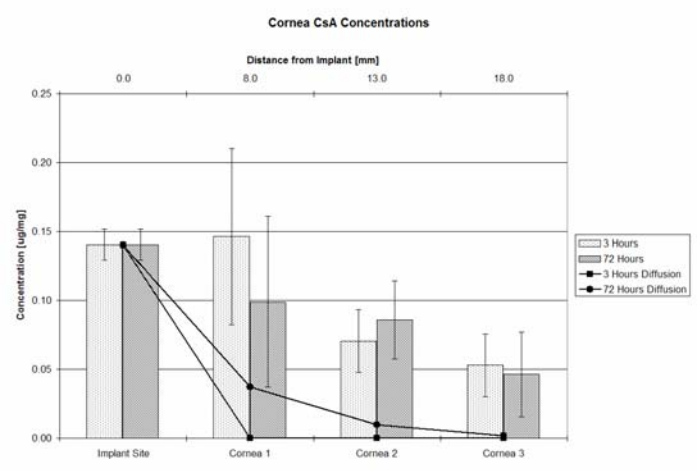

Figure 4-4: Cornea cyclosporine concentrations at increasing distances from the implant at 3 and 72 hours. The bars correspond to the experimentally measured cyclosporine concentrations at the corresponding sites on the cornea. The lines predict concentrations if drug dispersion in the cornea is due to diffusion alone as a function of distance.

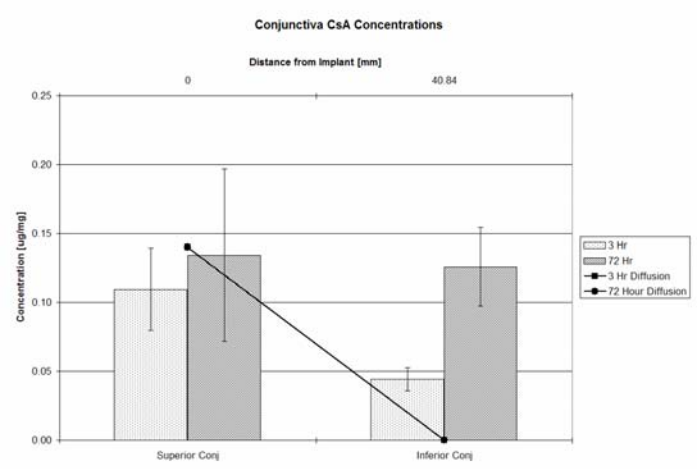

Figure 4-5: Conjunctival cyclosporine concentrations at increasing distances from the implant at 3 and 72 hours. The bars correspond to the experimentally measured cyclosporine concentrations at the corresponding sites on the conjunctiva. The lines predict concentrations due to drug diffusion across circular distances around the cornea, which were calculated based on the 13 mm radius from implant to the center of the cornea.

Long-term Pharmacokinetics

The right eyes of fifteen normal research beagles received a 0.75 inch CsA episcleral implant, and the beagles were euthanized at 1 month, 3 months, 6 months, 9 months, and 1 year for ocular drug extraction (Table 4-1). Corneal cyclosporine levels ranged from 0.18 ± 0.06 ug/mg to 0.009 ± 0.004 ug/mg during the 1 year study, but the corneal CsA concentration at 1 year was 0.04 ± 0.05 ug/mg. Aqueous humor levels at 1 year were at 0.007 ± 0.01 ug/mg, and the highest aqueous CsA concentration was

0.13 ± 0.15 ug/mg at 3 months. The conjunctival CsA concentrations ranged from 0.28 ± 0.35 ug/mg to 0.125 ± 0.05 ug/mg.

Table 4-1

Time	Lacrimal Gland		3E-Gland		Lens		Conjunctivae		Cornea		Sclerae	
[Months]	*Average*	*Std.Dev.*	*Average*	*Std.Dev.*	*Average*	*Std.Dev.*	*Average*	*Std.Dev.*	*Average*	*Std.Dev.*	*Average*	*Std.Dev.*
1	0.082	0.0984	0.188	0.0583	0.056	0.0214	0.234	0.0614	0.179	0.0647	0.225	0.0905
2	0.025	0.0047	0.188	0.0000	0.013	0.0090	0.128	0.0854	0.034	0.0022	0.086	0.0193
6	0.025	0.0166	0.056	0.0309	0.009	0.0078	0.125	0.0535	0.044	0.0166	0.102	0.0038
9	0.061	0.0392	0.105	0.0380	0.001	0.0003	0.279	0.3480	0.009	0.0040	0.044	0.0131
12	0.173	0.1782	0.074	0.0031	0.004	0.0026	0.163	0.0754	0.036	0.0469	0.075	0.0408

Time	Ciliary Body		Aqueous humor		Vitreous humor		Upper Eyelid		Lower Eyelid	
[Months]	*Average*	*Std.Dev.*	*Average*	*Std.Dev.*	*Average*	*Std.Dev.*	*Average*	*Std.Dev.*	*Average*	*Std.Dev.*
1	0.095	0.0356	0.104	0.0895	0.007	0.0008	0.171	0.1038	0.140	0.0631
2	0.054	0.0342	0.131	0.1479	0.001	0.0007	0.049	0.0250	0.040	0.0365
6	0.071	0.0263	0.006	0.0083	0.005	0.0006	0.056	0.0251	0.046	0.0023
9	0.058	0.0168	0.000	0.0000	0.017	0.0076	0.068	0.0632	0.083	0.0837
12	0.070	0.0245	0.007	0.0115	0.003	0.0007	0.098	0.0866	0.066	0.0657

Toxicity Evaluation

Six dogs each received 0.75 inch episcleral implant devices in one eye. Over the 1-year period, clinical examinations showed no signs of ocular toxicity (Figure 4-6). There were no significant changes in the ERG recordings compared to baseline during the 1-year study in both eyes (Figure 4-7). The histopathologic appearance by light microscopy in all eyes showed normal ocular tissues. There was a fine fibrous encapsulation surrounding the implant securing it to the episclera (Figure 4-8). There were no signs of retinal toxicity in all quadrants of the eye. In 2 of 6 dogs, there was a lymphoplasmacytic reaction around the implants; however, there was no observable swelling clinically.

Figure 4-6: Clinical examinations of beagles with episcleral implants were normal.

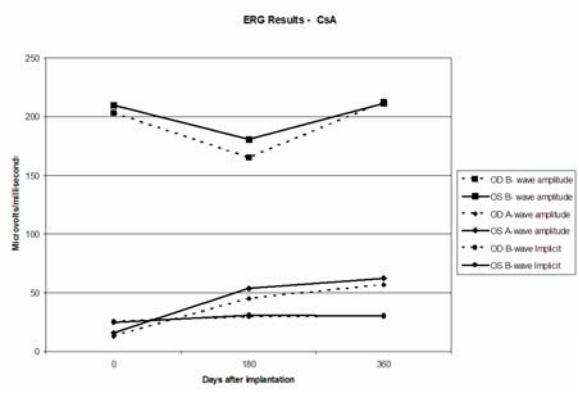

Figure 4-7: At 1 year, there were no significant changes from baseline in ERG results of beagles.

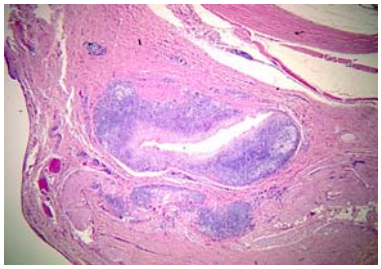

Figure 4-8: Light microscopy of histopathology in all eyes showed normal ocular tissues. There was a fine fibrous encapsulation surrounding the implant securing it to the episclera.

Discussion

In this study, a single episcleral implant delivered therapeutic CsA levels to the cornea as early as 3 hours, and continued to release therapeutic concentrations for 1 year in animals. CsA is therapeutic for preventing high-risk corneal graft rejection at concentrations that inhibit T-cell activation and vascular endothelial cell proliferation, which are 0.0001 – 0.001 ug/mg and 0.0012 – 0.06 ug/mg, respectively [127, 128] [129-135]. The corneal CsA concentrations were .09 ± .05 ug/mg at the 3 hour time point and remained above the therapeutic ranges at 1 year, when the concentration was 0.04 ± 0.05 ug/mg. Aqueous humor CsA concentrations were also well above the defined therapeutic range in both the short and long term experiments, suggesting sufficient penetration through all layers of the cornea as early as 3 hours and lasting for at least 1 year, as endothelial rejection is the most common type of allograft rejection [110]. The short time point experiments used the 0.5 inch episcleral

implants while the long time points obtained from beagle experiments used the 0.75 inch implants due to animal globe size. Nonetheless, the drug concentrations achieved from the two different lengths of implants are roughly comparable because they exhibited similar matrix style release kinetics, and demonstrated similar release rates for one year (Figure 4-3).

It is also important to suppress T-cell activation in the draining lymph nodes of eyes following a corneal allograft because the generation of an alloresponse occurs in these lymph nodes for both low and high-risk cases [136, 137]. The episcleral implant delivered concentrations of 0.1 ± 0.04 ug/mg and 0.12 ± 0.09 ug/mg of cyclosporine to the buccal lymph node of rabbits at 1 hour and 1 week respectively, which are 2 to 3 log units higher than the range necessary to inhibit T-cell activation in vitro. Furthermore, the delivery of antigen-presenting cells and antigenic material that stimulate the alloimmunization in draining lymph nodes and the influx of effector cells on the cornea that eventually lead to graft rejection is enabled by hem- and lymphangiogenesis at the graft site [138]. In high-risk corneal transplants, the host bed is often substantially vascularized with lymph and blood vessels, and inflamed, new blood and lymph vessel ingrowth begins soon after surgery [138]. Thus, it is also important to inhibit hem- and lymphangiogenesis to eliminate or reduce the afferent and efferent arms of the corneal allograft response that lead to rejection early. The episcleral implant delivers cyclosporine levels, as early as 3 hours, for 1 year to ocular tissues containing lymphatic and blood vessels within the range of vascular endothelial cell proliferation inhibition. The inhibition of lymph and blood vessel

growth is reversible upon cessation of cyclosporine therapy and is not cytoclastic, which avoids permanent vascular damage [134, 139, 140]. These levels of cyclosporine may cause the corneal lymph and blood vessels to regress and reestablish immunologic privilege.

The rapid rate that the episcleral implant delivered high concentrations of CsA to the cornea, conjunctiva, and buccal lymph node, suggests that diffusion may not be the only drug dispersion mechanism present. The CsA concentration (C) due to diffusion in one dimension and in the absence of clearance processes, can be predicted with the following equation[141]:

$C = C_o \text{erfc}\left[x / \left(2\sqrt{Dt}\right)\right]$, where C_o is the constant concentration in the tissue adjacent to the source (implant), *D* is the coefficient for solution diffusion through the tissue, t is time, erfc is the complementary error function, and *x* is the distance between the source and the measurement position. The coefficients for diffusion of cyclosporine through rabbit cornea and conjunctiva were estimated from measurements from literature of a wide range of hydrophilic and lipophilic model solutes to be 1.0×10^{-6} cm^2/sec and 4.4×10^{-7} cm^2/sec respectively[5, 142] [143] [2]. Contrastingly, when the experimental data is taken to be due to diffusion alone, the diffusion coefficient for diffusion of cyclosporine across the cornea is estimated to be 1.8 x 10^-2 cm^2/sec. The distances from the implant to the sampling site (*x*) on the cornea were 8, 13, and 18 mm, corresponding to the trephined sections of the cornea. For the conjunctiva, circular distances around the cornea were calculated based on the 13 mm radius (from implant to the center of the cornea) (Figure 4-2). The origin was taken to be at the

implant site in the superior conjunctiva giving $13\pi = 40.8$ mm as the location of the interior conjunctiva. The theoretical concentrations on the cornea due to diffusion alone were significantly less than the experimental concentrations ($p < 0.05$) at 13 and 18 mm away from the implant site at 3 and 72 hours (Figures 4-2 and 4-9). The inferior conjunctiva exhibited significantly higher CsA concentration at 72 hours than predicted for movement by diffusion alone.

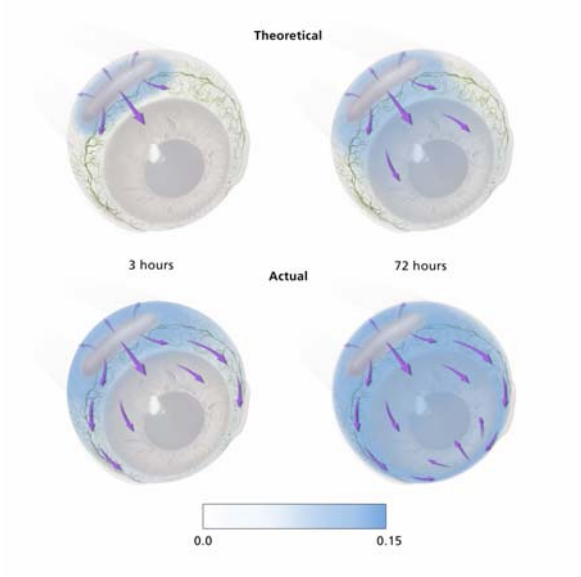

Figure 4-9: (Top) Theoretical drug concentrations due to diffusion alone at 3 hours (a) and 72 hours (a). (Bottom) Experimental drug concentrations at 3 hours (c) and 72 hours (d) imply that diffusion alone does not provide for the drug movement across the cornea.

Because high levels of CsA were detected in the buccal lymph node at 1 hour and 1 week, we hypothesize that conjunctival lymphatic vessels contribute to the rapid distribution of the drug around the cornea. Previous investigations of drug concentrations in the ipsilateral cervical lymph nodes have also shown significant lymphatic clearance from the sub-Tenon's space of small molecular weight hydrophilic compounds such as gadolinium-DTPA [60], and compounds as large as albumin [98-100]. The role of conjunctival lymphatics in drug delivery to the cornea was first suggested in 1957 by Sugar, when he proposed that the transfer of

subconjunctivally-injected substances reached the anterior chamber via conjunctival lymphatics [71]. It has also been suggested that the conjunctival lymphatics play a role in drug elimination from sub-Tenon's injections of triamcinolone acetonide. Robinson et al. showed that significant concentrations of drug entered the posterior segment only when the lymphatic circulation was eliminated at the injection site, because there was minimal lymphatic uptake of the drug to impede the transscleral diffusion [144]. In the current study, the ring of Orts, which is concentric with the cornea, and its afferent lymphatic vessels around the implant site absorb the cyclosporine near the implant site. The CsA is the transported out of the lymphatic vessels along its flow pathway around the cornea. Thus, the lymphatic flow surrounding the cornea may contribute to the rapid CsA dispersion across the cornea and conjunctiva. Further studies are necessary to support this hypothesis. Nonetheless, one should be cautious in using diffusion coefficients determined *in vitro* to predict drug transport *in vivo* which will neglect the contribution of other coexisting modes of drug transport, such as lymphatics.

In the literature, there are currently two cyclosporine releasing implants studied for the prevention of high risk corneal allograft rejection. Apel et al. studied a polylactic-glycolic acid (PLGA) disc-shaped CsA implant in a high risk rabbit model, and showed that these devices implanted at the time of transplantation improved the survival time of the grafts [122]. *In vitro*, these implants exhibited stable release for less than 100 days before reaching an unstable phase characterized by bulk degradation of PLGA. Unlike our episcleral implant, which maintained stable drug

release for 400 days, the *in vitro* release from PLGA are difficult to predict beyond the first 100 days. The corneal concentration achieved from the PLGA implant was 0.4 ng/mg at 35 days, which is below the therapeutic range for preventing PKP rejection and 3 log units lower than corneal CsA levels from episcleral implants at 42 days [89]. Xie et al. reported experiments with a CsA PLG implant that was implanted in the aqueous humor and subconjunctival region of rat models of PKP rejection [145]. Although the PLG delivery system significantly prolonged corneal allograft survival in a high-risk corneal graft rejection model in rats compared to controls, the CsA concentrations achieved were below the therapeutic range. Furthermore, even though the PLGA subconjunctival implant and the PLG implant are biodegradable, Apel at al. showed the bulk degradation of the polymer to be disadvantageous in generating a long term release profile. Silicone, the polymer in our episcleral implant has demonstrated to be non-bioreactive and exhibited prolonged steady release for over 1 year. The episcleral implant is also easily retrievable with minimal infection. Furthermore, the silicone drug matrix allows the episcleral implant to remain flexible to conform to the curvature of the globe, and no extrusions were observed in our long term animal experiments.

Several other drug delivery methods have been investigated for preventing corneal allograft rejection. Local injections into the subconjunctival space[146, 147], vitreous[148], and anterior chamber[149] have shown very low corneal levels and thus a short-lived therapeutic effect. Collagen shields and fragments appeared to be more effective than systemic formulations, however also had short-lived effects,

lasting for up to 12 hours only [150, 151]. Microspheres, liposomes, and nanocapsules also do not provide the prolonged release that prevention of high-risk corneal allografts require [28-33].

Our experiments have shown that episcleral implants are safe and effective at delivering therapeutic levels to the cornea and surrounding tissues for preventing corneal allograft rejection. The implant can be surgically placed on the episclera at the time of PKP, since the implant achieves therapeutic levels as early as 3 hours. Although these episcleral CsA implants are expected to be therapeutic, further studies are required to determine the effectiveness of these episcleral devices in PKP models.

Chapter 5: Conclusion and Future Directions

Conclusion

Recent advances in ocular drug delivery have had a profound impact in clinical ophthalmology, especially in the management of sight-threatening diseases. Understanding of the barriers and mechanisms of drug delivery provides the fundamental parameters of developing new therapies. The studies described in the previous chapters contribute to the field of ocular drug delivery as they describe the significance of the three types of transscleral drug transport barriers, and describe a drug-releasing implant for the prevention of high-risk PKP rejection. It is now understood that the most significant barrier to transscleral delivery may not be the scleral tissue or choroidal vasculature, as suggested in the literature [60, 87-89], but the conjunctival lymphatic and blood vessels. In addition, the pharmacokinetic studies of the episcleral implant suggested that a mechanism other than diffusion provided for rapid drug dispersion across the corneal tissue. Both of these studies suggest that conjunctival lymphatic vessels may play an important drug delivery role. It is important to further investigate the mechanisms that conjunctival lymphatics contribute to ocular pharmacokinetics drug delivery.

Future Directions

These studies point towards further elucidating the role of conjunctival lymphatics as a clearance mechanism in the eye. Real-time analysis should be performed, to see the dispersion from the sub-Tenon's space to various parts of the eye. An opaque tracer may be utilized to see where the solution is transported at various time points through the transparent conjunctiva. An alternative or additional real-time analysis of lymphatics may be magnetic resonance imaging. Furthermore, the drug dispersion that occurred across the cornea from the episcleral implant was in the lateral direction. Lateral drug diffusion of ocular tissues has not previously been studied, as past permeability studies were of molecules through tissues [4,5]. Finally, because the episcleral implant was demonstrated to be safe and effective at releasing therapeutic levels of CsA, animal models of PKP, as well as clinical studies should be performed. The future of ocular drug delivery will be finding ways to bypass and use the conjunctival lymphatic vessel flow to design more effective therapies.

Bibliography

1. Whitcher, J.P., M. Srinivasan, and M.P. Upadhyay, Corneal blindness: a global perspective. Bull World Health Organ, 2001. 79(3): p. 214-21.
2. Snell, R.S.L., Michael A., Clinical Anatomy of the Eye. 2 ed. 1998, Malden, MA: Blackwell Science, Inc.
3. Hosoya, K., V.H. Lee, and K.J. Kim, Roles of the conjunctiva in ocular drug delivery: a review of conjunctival transport mechanisms and their regulation. Eur J Pharm Biopharm, 2005. 60(2): p. 227-40.
4. Lawrence, M.S. and J.W. Miller, Ocular tissue permeabilities. Int Ophthalmol Clin, 2004. 44(3): p. 53-61.
5. Prausnitz, M.R. and J.S. Noonan, Permeability of cornea, sclera, and conjunctiva: a literature analysis for drug delivery to the eye. J Pharm Sci, 1998. 87: p. 1479-1488.
6. Lee, S.S., Yuan, P., Robinson, M.R., Ocular Implants for Drug Delivery, in Encyclopedia of Biomaterials and Biomedical Engineering, G.L. Bowlin, Wnek, G., Editor. 2004, Marcel Dekker: New York, NY. p. 1105-1118.
7. Yasukawa, T., et al., Drug delivery systems for vitreoretinal diseases. Prog Retin Eye Res, 2004. 23(3): p. 253-81.
8. Ambati, J. and A.P. Adamis, Transscleral drug delivery to the retina and choroid. Prog Retin Eye Res, 2002. 21(2): p. 145-51.
9. Hughes, P.M., et al., Topical and systemic drug delivery to the posterior segments. Adv Drug Deliv Rev, 2005. 57(14): p. 2010-32.
10. Donoso, L.A., et al., The role of inflammation in the pathogenesis of age-related macular degeneration. Surv Ophthalmol, 2006. 51(2): p. 137-52.
11. Friedman, D.S., et al., Prevalence of age-related macular degeneration in the United States. Arch Ophthalmol, 2004. 122(4): p. 564-72.
12. Kempen, J.H., et al., The prevalence of diabetic retinopathy among adults in the United States. Arch Ophthalmol, 2004. 122(4): p. 552-63.
13. Garg, P., et al., The value of corneal transplantation in reducing blindness. Eye, 2005. 19(10): p. 1106-14.
14. Fraunfelder, F.T., National Registry of Drug-Induced Ocular Side Effects. Am J Ophthalmol, 1990. 110(4): p. 426-7.
15. Geroski, D.H. and H.F. Edelhauser, Drug delivery for posterior segment eye disease. Invest Ophthalmol Vis Sci, 2000. 41(5): p. 961-4.
16. Lee, Y.C., P. Simamora, and S.H. Yalkowsky, Effect of Brij-78 on systemic delivery of insulin from an ocular device. J Pharm Sci, 1997. 86(4): p. 430-3.

17. Bernatchez, S.F., et al., Biocompatibility of a new semisolid bioerodible poly(ortho ester) intended for the ocular delivery of 5-fluorouracil. J Biomed Mater Res, 1994. 28(9): p. 1037-46.

18. Mochizuki, K., et al., Retinal toxicity of antibiotics: evaluation by electroretinogram. Doc Ophthalmol, 1988. 69(2): p. 195-202.

19. Peyman, G.A. and J.A. Schulman, Intravitreal drug therapy. Jpn J Ophthalmol, 1989. 33(4): p. 392-404.

20. Hainsworth, D.P., et al., Intravitreal delivery of ciprofloxacin. J Ocul Pharmacol Ther, 1996. 12(2): p. 183-91.

21. Heinemann, M.H., Staphylococcus epidermidis endophthalmitis complicating intravitreal antiviral therapy of cytomegalovirus retinitis. Case report. Arch Ophthalmol, 1989. 107(5): p. 643-4.

22. Brown, G.C., et al., Retinal toxicity of intravitreal gentamicin. Arch Ophthalmol, 1990. 108(12): p. 1740-4.

23. Seawright, A.A., R.D. Bourke, and R.J. Cooling, Macula toxicity after intravitreal amikacin. Aust N Z J Ophthalmol, 1996. 24(2): p. 143-6.

24. Cruysberg, L.P., et al., In vitro human scleral permeability of fluorescein, dexamethasone-fluorescein, methotrexate-fluorescein and rhodamine 6G and the use of a coated coil as a new drug delivery system. J Ocul Pharmacol Ther, 2002. 18(6): p. 559-69.

25. Cruysberg, L.P.J., et al., Effective Transscleral Delivery of Two Retinal Anti-Angiogenic Molecules: Carboxyamido-triazole (CAI) and 2-Methoxyestradiol (2ME2). Retina (in press), 2005.

26. Dahr, S.S., et al., Anterior Subtenon's Triamcinolone Acetonide (ASTA) Injection for the Treatment of Diabetic Macular Edema: 4 to 6 Month Clinical Followup. Invest Ophthalmol Vis Sci, 2005. 46: p. ARVO E-Abstract 1431.

27. Brancato, R., et al., Diabetic Macular Edema: Juxtascleral (JS) versus Intravitreal (IV) Triamcinolone Acetonide (TA) Injections. Invest Ophthalmol Vis Sci, 2005. 46(ARVO E-Abstract 281).

28. Vallelado, A.I., et al., Efficacy and safety of microspheres of cyclosporin A, a new systemic formulation, to prevent corneal graft rejection in rats. Curr Eye Res, 2002. 24(1): p. 39-45.

29. de Rojas Silva, M.V., et al., Efficacy of subconjunctival cyclosporin-containing microspheres on keratoplasty rejection in the rabbit. Graefes Arch Clin Exp Ophthalmol, 1999. 237(10): p. 840-7.

30. Milani, J.K., et al., Prolongation of corneal allograft survival with liposome-encapsulated cyclosporine in the rat eye. Ophthalmology, 1993. 100(6): p. 890-6.

31. Alghadyan, A.A., et al., Liposome-bound cyclosporine: clearance after intravitreal injection. Int Ophthalmol, 1988. 12(2): p. 109-112.

32. Pleyer, U., et al., Ocular absorption of cyclosporine A from liposomes incorporated into collagen shields. Curr Eye Res, 1994. 13(3): p. 177-81.

33. Juberias, J.R., et al., Efficacy of topical cyclosporine-loaded nanocapsules on keratoplasty rejection in the rat. Curr Eye Res, 1998. 17(1): p. 39-46.

34. Kaur, I.P., et al., Vesicular systems in ocular drug delivery: an overview. Int J Pharm, 2004. 269(1): p. 1-14.

35. Musch, D.C., et al., Treatment of cytomegalovirus retinitis with a sustained-release ganciclovir implant. The Ganciclovir Implant Study Group. N Engl J Med, 1997. 337: p. 83-90.

36. Taylor, S.A., S.M. Galbraith, and R.P. Mills, Causes of non-compliance with drug regimens in glaucoma patients: a qualitative study. J Ocul Pharmacol Ther, 2002. 18(5): p. 401-9.

37. Olsen, T.W., et al., Human sclera: thickness and surface area. Am J Ophthalmol, 1998. 125: p. 237-41.

38. Ambati, J., et al., Diffusion of high molecular weight compounds through sclera. Invest Ophthalmol Vis Sci, 2000. 41(5): p. 1181-1185.

39. Ambati, J., et al., Transscleral delivery of bioactive protein to the choroid and retina. Invest Ophthalmol Vis Sci, 2000. 41(5): p. 1186-91.

40. Ross, M.L., P. Yuan, and M.R. Robinson, Intraocular Drug Delivery Implants. Review of Ophthalmology, 2000: p. 95-99.

41. Metrikin, D.C. and R. Anand, Intravitreal drug administration with depot devices. Curr Opin Ophthalmol, 1994. 5(3): p. 21-9.

42. Morita, Y., et al., Intravitreous delivery of dexamethasone sodium m-sulfobenzoate from poly(DL-lactic acid) implants. Biol Pharm Bull, 1998. 21(2): p. 188-90.

43. Kunou, N., et al., Long-term sustained release of ganciclovir from biodegradable scleral implant for the treatment of cytomegalovirus retinitis. J Control Release, 2000. 68(2): p. 263-71.

44. Wang, G., et al., In vitro and in vivo evaluation in rabbits of a controlled release 5-fluorouracil subconjunctival implant based on poly(D,L-lactide-co-glycolide). Pharm Res, 1996. 13(7): p. 1059-64.

45. Shell, J.W., Ophthalmic drug delivery systems. Surv Ophthalmol, 1984. 29(2): p. 117-28.

46. Robinson, M.R., et al., Safety and pharmacokinetics of intravitreal 2-methoxyestradiol implants in normal rabbit and pharmacodynamics in a rat model of choroidal neovascularization. Exp Eye Res, 2002. 74(2): p. 309-17.

47. Quigley, H.A., I.P. Pollack, and T.S. Harbin, Jr., Pilocarpine ocuserts. Long-term clinical trials and selected pharmacodynamics. Arch Ophthalmol, 1975. 93(9): p. 771-5.

48. Hitchings, R.A. and R.J. Smith, Experience with pilocarpine Ocuserts. Trans Ophthalmol Soc U K, 1977. 97(1): p. 202-5.

49. Ashton, P., et al., Review: implants. J Ocul Pharmacol, 1994. 10(4): p. 691-701.

50. Anand, R., et al., Control of cytomegalovirus retinitis using sustained release of intraocular ganciclovir. Arch Ophthalmol, 1993. 111(2): p. 223-227.

51. Smith, T.J., et al., Intravitreal sustained-release ganciclovir. Arch Ophthalmol, 1992. 110(2): p. 255-8.

52. Martin, D.F., et al., Treatment of cytomegalovirus retinitis with an intraocular sustained- release ganciclovir implant. A randomized controlled clinical trial. Arch Ophthalmol, 1994. 112(12): p. 1531-1539.

53. Musch, D.C., et al., Treatment of cytomegalovirus retinitis with a sustained-release ganciclovir implant. The Ganciclovir Implant Study Group. N Engl J Med, 1997. 337(2): p. 83-90.

54. Sutter, F.K. and M.C. Gillies, Pseudo-endophthalmitis after intravitreal injection of triamcinolone. Br J Ophthalmol, 2003. 87(8): p. 972-4.

55. Nelson, M.L., et al., Infectious and presumed noninfectious endophthalmitis after intravitreal triamcinolone acetonide injection. Retina, 2003. 23(5): p. 686-91.

56. Parke, D.W., Intravitreal triamcinolone and endophthalmitis. Am J Ophthalmol, 2003. 136(5): p. 918-9.

57. Moshfeghi, A.A., et al., Pseudohypopyon after intravitreal triamcinolone acetonide injection for cystoid macular edema. Am J Ophthalmol, 2004. 138(3): p. 489-92.

58. Ozkiris, A. and K. Erkilic, Complications of intravitreal injection of triamcinolone acetonide. Can J Ophthalmol, 2005. 40(1): p. 63-8.

59. Li, S.K., S.A. Molokhia, and E.K. Jeong, Assessment of subconjunctival delivery with model ionic permeants and magnetic resonance imaging. Pharm Res, 2004. 21(12): p. 2175-84.

60. Kim, H., et al., Controlled drug release from an ocular implant: An evaluation using dynamic three-dimensional MRI. Invest Ophthalmol Vis Sci, 2004. 45: p. 2722-2731.

61. Jakobiec, F.A., et al., Combined surgery and cryotherapy for diffuse malignant melanoma of the conjunctiva. Arch Ophthalmol, 1980. 98: p. 1390-1396.

62. Wilkes, T.D. and F.T. Fraunfelder, Principles of cryotherapy. Ophthalmic Surg, 1979. 10: p. 21-30.

63. Brownstein, S., et al., Cryotherapy for precancerous melanosis (atypical melanocytic hyperplasia) of the conjunctiva. Arch Ophthalmol, 1981. 99: p. 1224-1231.

64. Suomalainen, V.P., Comparison of retinal lesions produced by transscleral krypton laser photocoagulation, transpupillar krypton laser photocoagulation and cryocoagulation. Acta Ophthalmol (Copenh), 1993. 71(2): p. 224-9.

65. Olsen, T.W., et al., Human scleral permeability: effects of age, cryotherapy, transscleral diode laser, and surgical thinning. Invest Ophthalmol Vis Sci, 1995. 36: p. 1893-1903.

66. Sullivan, J.H., Cryosurgery in Ophthalmic Practice. Ophthalmic Surg, 1979. 10: p. 37-41.

67. Steel, D.H., J. West, and W.G. Campbell, A randomized controlled study of the use of transscleral diode laser and cryotherapy in the management of rhegmatogenous retinal detachment. Retina, 2000. 20(4): p. 346-57.

68. Friedrichsen, E.J., et al., Immunohistochemical comparison of transscleral continuous wave 1064-Nd:YAG laser retinopexy and cryoretinopexy. Retina, 1994. 14(1): p. 51-8.

69. Dunker, S., et al., The effect of retinal cryoapplication on the vitreous. Retina, 1997. 17(4): p. 338-43.

70. Gray, H., VIII. The Lymphatic System, in Anatomy of the Human Body, H. Gray, Editor. 1918, Lea & Febiger: Philadelphia. p. 1-41.

71. Sugar, H.S., A. Riazi, and R. Schaffner, The bulbar conjunctival lymphatics. Trans Am Acad Ophthalmol Otolaryngol, 1957. 39: p. 212-223.

72. Duke-Elder, S. and D.M. Maurice, Symbols of ocular dynamics. Br J Ophthalmol, 1957. 41: p. 702-702.

73. Collin, H.B., Ocular lymphatics. Am J Optom Arch Am Acad Optom, 1966. 43(2): p. 96-106.

74. Duke-Elder, S. and K.C. Wybar, The anatomy of the visual system, in System of Ophthalmology, S. Duke-Elder, Editor. 1961, The C.V. Mosby Co.: St. Loius. p. 541-555.

75. Price, N.C., R.J. Cooling, and N.C. Andrew, The role of vitrectomy following accidental intraocular injection of deposteroid preparations. Trans Ophthalmol Soc U K, 1986. 105 (Pt 4): p. 469-72.

76. Watson, P.G. and R.D. Young, Scleral structure, organisation and disease. A review. Exp Eye Res, 2004. 78(3): p. 609-23.

77. Velez, G., et al., Pharmacokinetics and toxicity of intravitreal chemotherapy for primary intraocular lymphoma. Arch Ophthalmol, 2001. 119(10): p. 1518-24.

78. Kim, H., et al., Controlled drug release from an ocular implant: an evaluation using dynamic three-dimensional magnetic resonance imaging. Invest Ophthalmol Vis Sci, 2004. 45(8): p. 2722-31.

79. Derendorf, H., et al., Pharmacokinetics and pharmacodynamics of glucocorticoid suspensions after intra-articular administration. Clin Pharmacol Ther, 1986. 39(3): p. 313-7.

80. Robinson, M.R., et al., Preclinical evaluation of a triamcinolone acetonide preservative-free (TAC-PF) formulation for intravitreal injection. Invest Ophthalmol Vis Sci, 2004. 45: p. ARVO E-Abstract 5058.

81. Jaffe, G.J., et al., Safety and pharmacokinetics of an intraocular fluocinolone acetonide sustained delivery device. Invest Ophthalmol Vis Sci, 2000. 41(11): p. 3569-3575.

82. Inoue, M., et al., Vitreous concentrations of triamcinolone acetonide in human eyes after intravitreal or subtenon injection. Am J Ophthalmol, 2004. 138(6): p. 1046-8.

83. Thomas, E. and D.P. Hainsworth, Intravitreal Concentration of Sub-Tenon's Injected Triamcinolone Acetonide. Invest Ophthalmol Vis Sci, 2005. 46: p. ARVO E-Abstract 5394.

84. Hyndiuk, R.A., Radioactive depot-corticosteroid penetration into monkey ocular tissue. II. Subconjunctival administration. Arch Ophthalmol, 1969. 82(2): p. 259-63.

85. Csaky, K.G., et al., Anterior Subtenon's Triamcinolone Acetonide (ASTTA) Injection for the Treatment of Diabetic Macular Edema: Animal and Clinical Findings. Invest Ophthalmol Vis Sci, 2005. 46: p. ARVO E-Abstract 4670.

86. Kalina, P.H., J.C. Erie, and L. Rosenbaum, Biochemical quantification of triamcinolone in subconjunctival depots. Arch Ophthalmol, 1995. 113(7): p. 867-9.

87. Moseley, H. and W.S. Foulds, The movement of xenon-133 from the vitreous to the choroid. Exp Eye Res, 1982. 34(2): p. 169-79.

88. Moseley, H., et al., Routes of clearance of radioactive water from the rabbit vitreous. Br J Ophthalmol, 1984. 68(3): p. 145-51.

89. Kim, H., et al., Preclinical evaluation of a novel episcleral cyclosporine implant for ocular graft-versus-host disease. Invest Ophthalmol Vis Sci, 2005. 46(2): p. 655-62.

90. Deak, S.T. and T.Z. Csaky, Factors regulating the exchange of nutrients and drugs between lymph and blood in the small intestine. Microcirculation, Endothelium, and Lymphatics, 1984. 1: p. 569-588.

91. Charman, W.N. and V.J. Stella, Anatomy and Physiology of the Lymphatics, in Lymphatic Transport of Drugs, W.N. Charman and V.J. Stella, Editors. 1992, CRC Press: Boca Raton. p. 1-36.

92. Leak, L.V., Lymphatic removal of fluids and particles in the mammalian lung. Environ Health Perspect, 1980. 35: p. 55-76.

93. Takada, K., et al., Biological and pharmaceutical factors affecting the absorption and lymphatic delivery of ciclosporin A from gastrointestinal tract. J Pharmacobiodyn, 1988. 11(2): p. 80-7.

94. Porter, C.J., Drug delivery to the lymphatic system. Crit Rev Ther Drug Carrier Syst, 1997. 14(4): p. 333-93.

95. Swartz, M.A., The physiology of the lymphatic system. Adv Drug Deliv Rev, 2001. 50(1-2): p. 3-20.

96. Kim, H., et al., Study of ocular transport of drugs released from an intravitreal implant using magnetic resonance imaging. Ann Biomed Eng, 2005. 33(2): p. 150-64.

97. Lee, S.S., et al., The Pharmacokinetics of a Novel Episcleral Cyclosporine Implant for High-Risk Keratoplasties. Invest Ophthalmol Vis Sci, 2005. 46: p. ARVO E-Abstract 2704.

98. Bill, A., The albumin exchange in the rabbit eye. Acta Physiol. Scand., 1964. 60: p. 18-29.

99. Bill, A., The Drainage of Albumin from the Uvea. Exp Eye Res, 1964. 75: p. 179-187.

100. Gruntzig, J., H. Schicha, and F. Huth, Eye and lymph drainage. Z Lymphol, 1979. 3: p. 35-45.

101. Boulton, M., et al., Lymphatic drainage of the CNS: effects of lymphatic diversion/ligation on CSF protein transport to plasma. Am J Physiol, 1997. 272(5 Pt 2): p. R1613-9.

102. Boulton, M., et al., Drainage of CSF through lymphatic pathways and arachnoid villi in sheep: measurement of 125I-albumin clearance. Neuropathol Appl Neurobiol, 1996. 22(4): p. 325-33.

103. Edelhauser, H.F. and T.H. Maren, Permeability of human cornea and sclera to sulfonamide carbonic anhydrase inhibitors. Arch Ophthalmol, 1988. 106: p. 1110-1115.

104. Cheruva, N.P.S., E.R. Escobar, and U.B. Kompella, Transscleral Transport: Barrier Properties of Sclera, Choroid-Tapetum, and Retinal Pigment Epithelium. Invest Ophthalmol Vis Sci, 2005. 46: p. ARVO E-Abstract 5390.

105. Peiffer, R.L., L. Pohm-Thorsen, and K. Corcoran, Models in Ophthalmology and Vision Research, in The Biology of the Laboratory Rabbit, P.J. Manning, D.H. Ringler, and C.E. Newcomer, Editors. 1994, Academic Press: San Diego. p. 409-433.

106. Prince, J.H., et al., Anatomy and Histology of the Eye and Orbit in Domestic Animals. 1960, Springfield: Charles C. Thomas- Publisher. 278-287.

107. Alm, A. and A. Bill, Ocular and optic nerve flow at normal and increased intraocular pressures in monkeys (Macaca irus); a study with radioactively

labelled microspheres including flow determinations in brain and some other tissues. Exp Eye Res, 1973. 15: p. 15-29.

108. Bill, A. and J. Stjernschantz, Cholinergic vasoconstrictor effects on the rabbit eye: Vasomotor effects of pentobarbital anesthesia. Acta Physiol. Scand., 1980. 108: p. 419-424.

109. Williams, K.A., et al., Long-term outcome in corneal allotransplantation. The Australian Corneal Graft Registry. Transplant Proc, 1997. 29(1-2): p. 983.

110. Larkin, D.F., Corneal allograft rejection. Br J Ophthalmol, 1994. 78(8): p. 649-52.

111. Zhao, J.C. and X.Y. Jin, Local therapy of corneal allograft rejection with cyclosporine. Am J Ophthalmol, 1995. 119(2): p. 189-94.

112. Borel, J.F., et al., Biological effects of cyclosporin A: a new antilymphocytic agent. Agents Actions, 1976. 6(4): p. 468-75.

113. Hill, J.C., The use of cyclosporine in high-risk keratoplasty. Am J Ophthalmol, 1989. 107(5): p. 506-10.

114. Busauschina, A., P. Schnuelle, and F.J. van der Woude, Cyclosporine nephrotoxicity. Transplant Proc, 2004. 36(2 Suppl): p. 229S-233S.

115. Graham, R.M., Cyclosporine: mechanisms of action and toxicity. Cleve Clin J Med, 1994. 61(4): p. 308-13.

116. Acheampong, A.A., et al., Distribution of cyclosporin A in ocular tissues after topical administration to albino rabbits and beagle dogs. Curr Eye Res, 1999. 18(2): p. 91-103.

117. BenEzra, D. and G. Maftzir, Ocular penetration of cyclosporin A. The rabbit eye. Invest Ophthalmol Vis Sci, 1990. 31(7): p. 1362-6.

118. Perry, H.D., et al., Topical Cyclosporine A in the management of postkeratoplasty glaucoma and corticosteroid-induced ocular hypertension (CIOH) and the penetration of topical 0.5% cyclosporine A into the cornea and anterior chamber. Clao J, 1998. 24(3): p. 159-65.

119. Bellot, J.L., et al., Corneal concentration and systemic absorption of cyclosporin-A following its topical application in the rabbit eye. Ophthalmic Res, 1992. 24(6): p. 351-6.

120. Vernillet, L., et al., Ocular distribution of cyclosporin A (Sandimmun) following systemic and topical administration to rabbits. Eur J Drug Metab Pharmacokinet, 1991. Spec No 3: p. 150-158.

121. Althaus, C., et al., Cyclosporin-A and its metabolites in the anterior chamber after topical and systemic application as determined with high-performance liquid chromatography-electrospray mass spectrometry. Ger J Ophthalmol, 1996. 5(4): p. 189-94.

122. Apel, A., et al., A subconjunctival degradable implant for cyclosporine delivery in corneal transplant therapy. Curr Eye Res, 1995. 14(8): p. 659-667.

123. Davis, J.L., B.C. Gilger, and M.R. Robinson, Novel approaches to ocular drug delivery. Curr Opin Mol Ther, 2004. 6(2): p. 195-205.

124. Robinson, M.R., et al., Ocular Therapeutic Agent Delivery Devices and Methods for Making and Using Same. Federal Register, 2001. 66: p. 29153-29155.

125. Miller, R.a.D., JE, Intracellular responses of the Muller (glial) cells of mudpuppy retina: their relation to the b-wave of the electroretinogram. J. Neurophysiol., 1970. 67: p. 442-448.

126. Baker, R.W., Controlled Release of Biologically Active Agents. 1987, New York: John Wiley and Sons.

127. Laferty, K.F., J.F. Borel, and P. Hodgkin, Cyclosporine-A (CsA): models for the mechanism of action. Tranplant Proc., 1983. 15: p. 2242-2247.

128. Keown, P.A. and C.R. Stiller, Cyclosporine: a double-edged sword. Hosp Pract (Off Ed), 1987. 22(5): p. 207-15, 219-20.

129. Zoja, C., et al., Cyclosporin-induced endothelial cell injury. Lab Invest, 1986. 55(4): p. 455-62.

130. Waldman, W.J., et al., Inhibition of angiogenesis-related endothelial activity by the experimental immunosuppressive agent leflunomide. Transplantation, 2001. 72(9): p. 1578-82.

131. Storogenko, M., et al., Cyclosporin-A inhibits human endothelial cells proliferation through interleukin-6-dependent mechanisms. Life Sci, 1997. 60(17): p. 1487-96.

132. Trapp, A. and M. Weis, The impact of immunosuppression on endothelial function. J Cardiovasc Pharmacol, 2005. 45(1): p. 81-7.

133. Dzirlo-Todorovic, J., [The effect of cyclosporine on human endothelial cells in culture]. Med Arh, 1998. 52(4): p. 195-8.

134. Iurlaro, M., et al., Antiangiogenesis by cyclosporine. Exp Hematol, 1998. 26(13): p. 1215-22.

135. Ferns, G., M. Reidy, and R. Ross, Vascular effects of cyclosporine A in vivo and in vitro. Am J Pathol, 1990. 137(2): p. 403-13.

136. Yamagami, S. and M.R. Dana, The critical role of lymph nodes in corneal alloimmunization and graft rejection. Invest Ophthalmol Vis Sci, 2001. 42(6): p. 1293-8.

137. Yamagami, S., M.R. Dana, and T. Tsuru, Draining lymph nodes play an essential role in alloimmunity generated in response to high-risk corneal transplantation. Cornea, 2002. 21(4): p. 405-9.

138. Cursiefen, C., et al., Corneal lymphangiogenesis: evidence, mechanisms, and implications for corneal transplant immunology. Cornea, 2003. 22(3): p. 273-81.

139. Seki, Y., et al., In vitro effect of cyclosporin A, mitomycin C and prednisolone on cell kinetics in cultured human umbilical vein endothelial cells. Thromb Res, 2005. 115(3): p. 219-28.

140. Lau, D.C., K.L. Wong, and W.S. Hwang, Cyclosporine toxicity on cultured rat microvascular endothelial cells. Kidney Int, 1989. 35(2): p. 604-13.

141. Crank, J., The Mathematics of Diffusion. 2nd ed. 1975, Oxford: Oxford University Press. 20-21.

142. Boubriak, O.A., et al., The effect of hydration and matrix composition on solute diffusion in rabbit sclera. Exp Eye Res, 2000. 71: p. 503-514.

143. Hamalainen, K.M., et al., Characterization of paracellular and aqueous penetration routes in cornea, conjunctiva, and sclera. Invest Ophthalmol Vis Sci, 1997. 38(3): p. 627-34.

144. Robinson, M.R., et al., A rabbit model for assessing the ocular barriers to the transscleral delivery of triamcinolone acetonide. Exp Eye Res, 2005.

145. Xie, L., et al., Prolongation of corneal allograft survival using cyclosporine in a polylactide-co-glycolide polymer. Cornea, 2001. 20(7): p. 748-52.

146. Behrens-Baumann, W., et al., Ciclosporin concentration in the rabbit aqueous humor and cornea following subconjunctival administration. Importance of anatomical site of injection. Graefes Arch Clin Exp Ophthalmol, 1986. 224(4): p. 368-70.

147. Kalsi, G.S., et al., Ocular pharmacokinetics of subconjunctivally administered cyclosporine in the rabbit. Can J Ophthalmol, 1991. 26(4): p. 200-5.

148. Pearson, P.A., et al., Evaluation of a delivery system providing long-term release of cyclosporine. Arch Ophthalmol, 1996. 114(3): p. 311-317.

149. Oh, C., et al., Local efficacy of cyclosporine in corneal transplant therapy. Curr Eye Res, 1994. 13(5): p. 337-343.

150. Mahlberg, K., R.J. Uusitalo, and O. Oksala, Prevention of high risk corneal graft rejection using cyclosporine A (CsA) incorporated into a collagen matrix. Ocul Immunol Inflamm, 1997. 5(2): p. 101-10.

151. Kanpolat, A., et al., Penetration of cyclosporin A into the rabbit cornea and aqueous humor after topical drop and collagen shield administration. Clao J, 1994. 20(2): p. 119-22.